INFN NAPOLI
Istituto Nazionale di Fisica Nucleare
Sezione di Napoli

Neutral current *B*-decay anomalies

Siavash Neshatpour
INFN, Sezione di Napoli

In collaboration with T. Hurth, N. Mahmoudi, D. Martinez Santos

Based on: [arXiv:1904.08399, arXiv:2012.12207 and arXiv:2104.10058]

8th Workshop on Theory, Phenomenology and Experiments in Flavour Physics
FPCapri2022

June 11 – 13, 2022

$b \to s\ell\ell$ anomalies

Several deviations ("anomalies") with respect to the SM predictions in $b \to s\ell\ell$ measurements

- P_5' $(B \to K^*\mu^+\mu^-)$: Long standing tension since 2013
  - 2020 LHCb update with 4.7 fb^{-1} [PRL 125, 011802 (2021)]

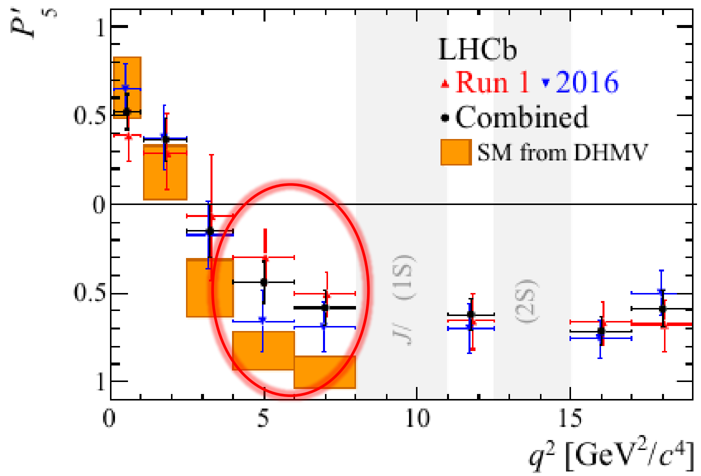

➢ $\approx 2.9\sigma$ local tension

⟶ significance depends on estimation of hadronic contributions

- First measurement of $B^+ \to K^{*+}\mu^+\mu^-$ angular observables
  - full Run 1 and Run 2 dataset with 9 fb^{-1} [PRL 126, 161802 (2021)]

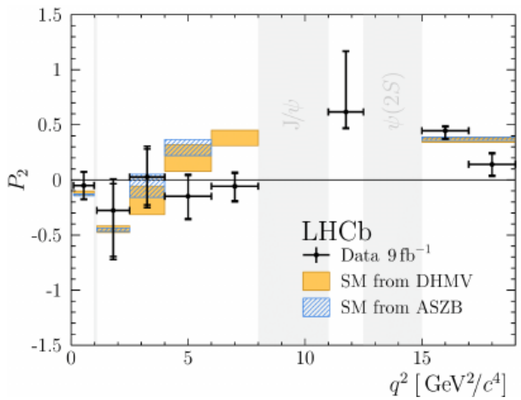

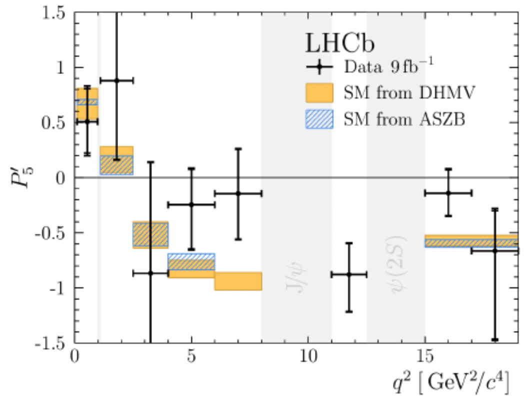

➢ overall results confirm the trend of tension with respect to the SM

Several deviations ("anomalies") with respect to the SM predictions in $b \to s\ell\ell$ measurements

- Branching fractions

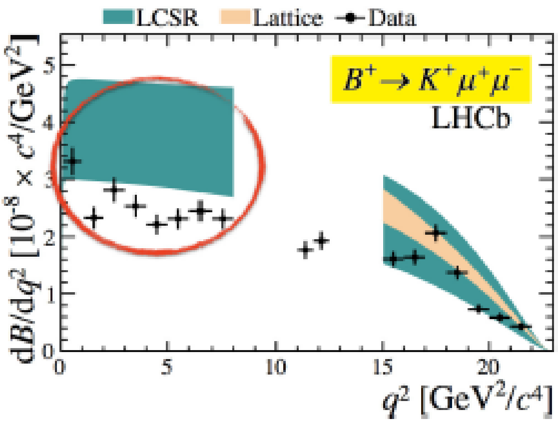

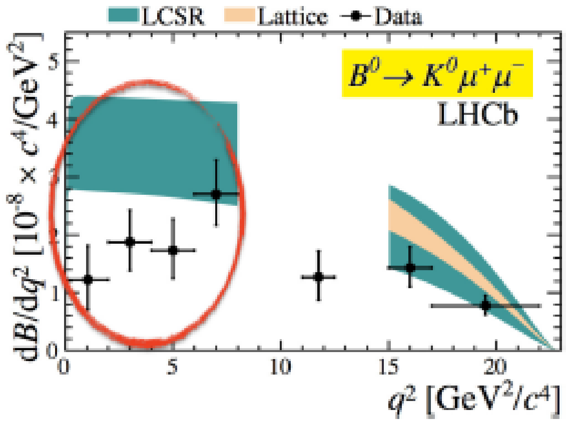

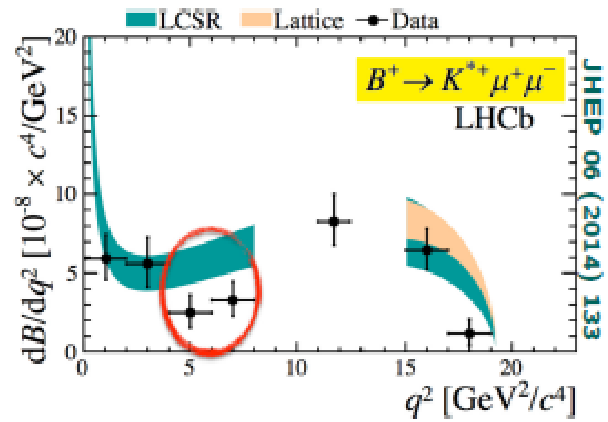

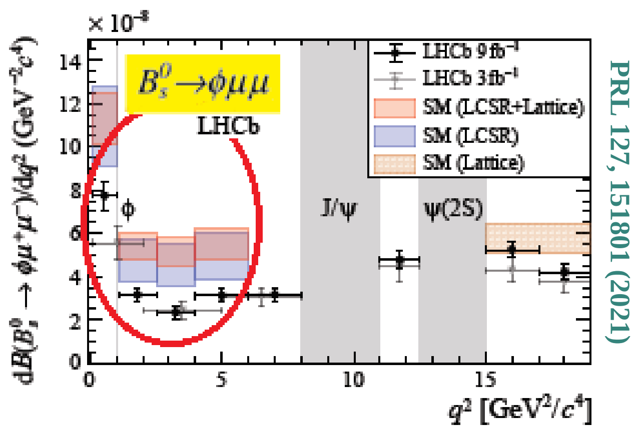

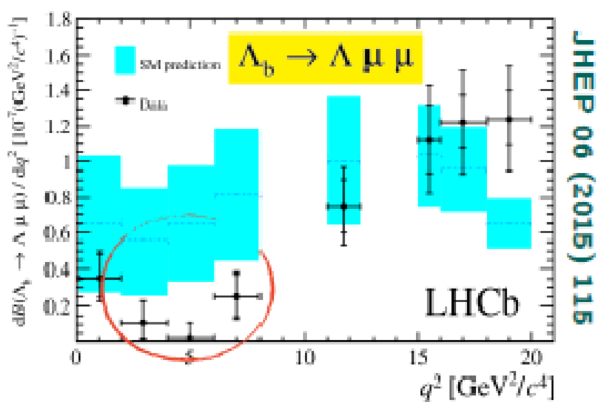

- Measurements below SM predictions with $\sim 2-3\sigma$ significance
- Large theory uncertainties (several form factors involved)

- Lepton flavour universality violating ratios $R_{K^{(*)}} \equiv \frac{BR(B \to K^{(*)}\mu^+\mu^-)}{BR(B \to K^{(*)}e^+e^-)}$

  - LHCb (3 fb^{-1}) April 2017:

  - LHCb (1 fb^{-1}) June 2014:
  - LHCb (5 fb^{-1}) March 2019:
  - LHCb (9 fb^{-1}) March 2021

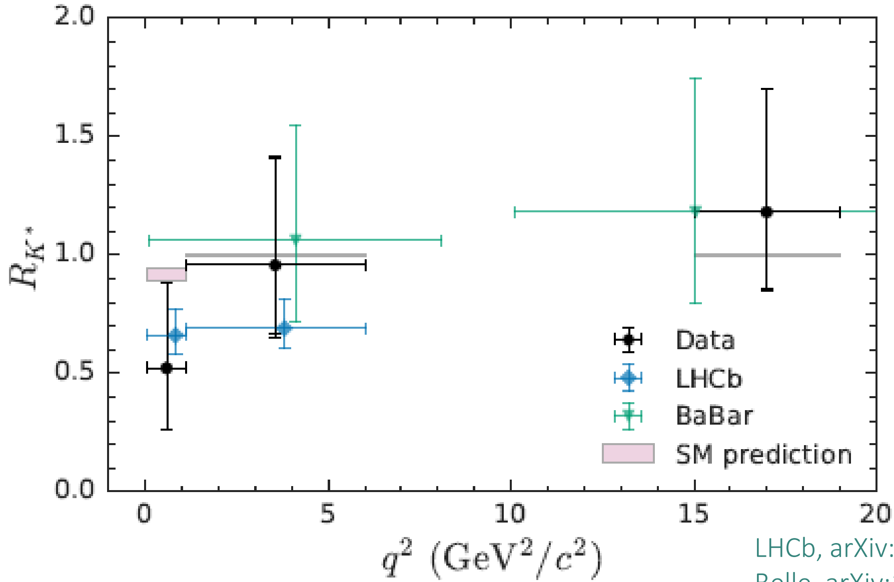

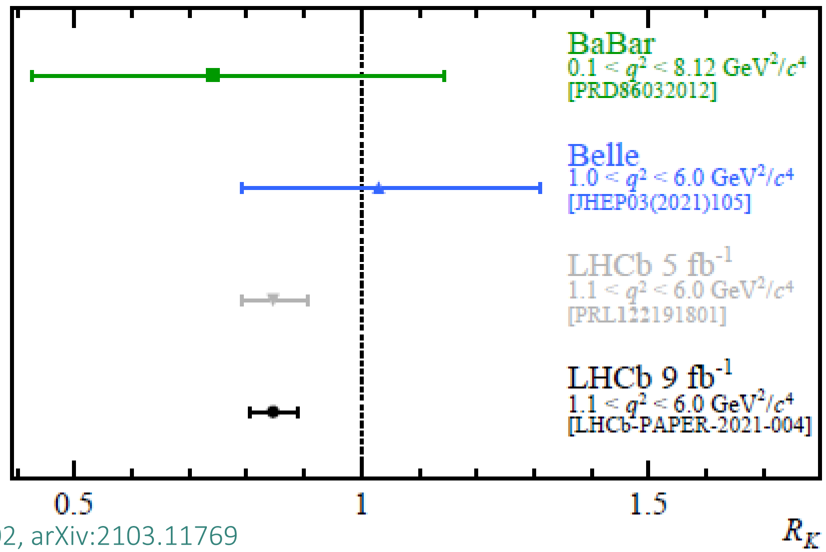

LHCb, arXiv:1705.05802, arXiv:2103.11769
Belle, arXiv:1904.02440, arXiv:1908.01848

- SM prediction very accurate with uncertainty less than (3%) 1%
- LHCb measurement below SM with (2.3σ) & 2.5σ for R_{K^*} and 3.1σ for R_K $\longrightarrow$ #cautiouslyexcited

- Lepton flavour universality violating ratios $R_{K_S^0\,(K^{*+})} \equiv \frac{BR(B\to K_S^0\,(K^{*+})\mu^+\mu^-)}{BR(B\to K_S^0\,(K^{*+})e^+e^-)}$

■ LHCb (9 fb^{-1}) October 2021

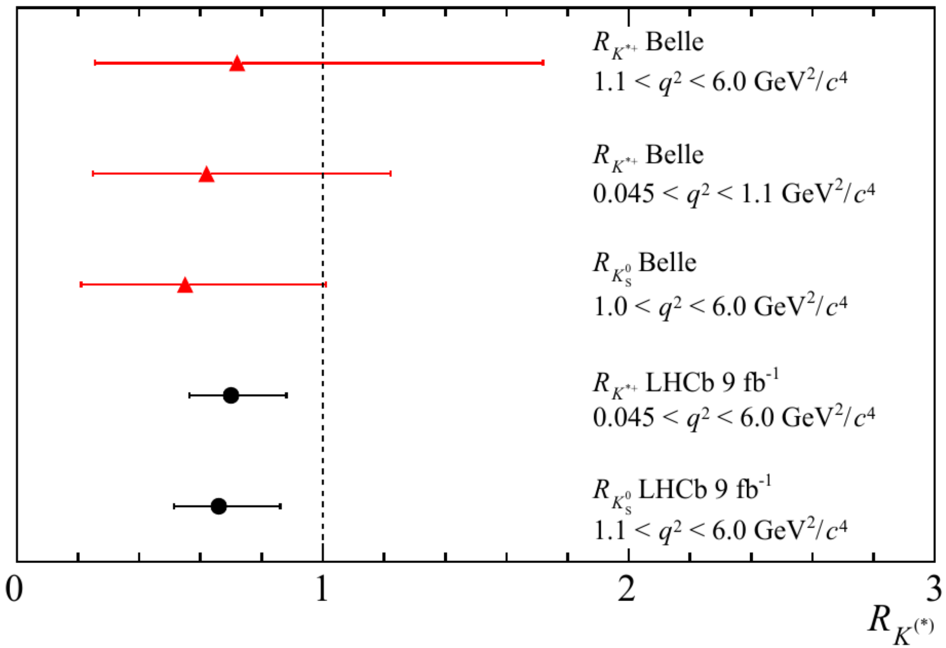

LHCb, arXiv:2110.09501
Belle, arXiv:1904.02440,
Belle,arXiv:1908.01848

- SM prediction very accurate with uncertainty less than 1%
- LHCb measurement only slightly below SM with less than 2σ but consistent with the trend observed in their isospin partners

BR($B \to \mu^+\mu^-$)

Combination of LHCb, CMS and ATLAS measurement for BR($B_{s,d} \to \mu^+\mu^-$)

- LHCb (9 $\mathbf{fb}^{-1}$) March 2021
  [PRD 105 (2022) 012010]

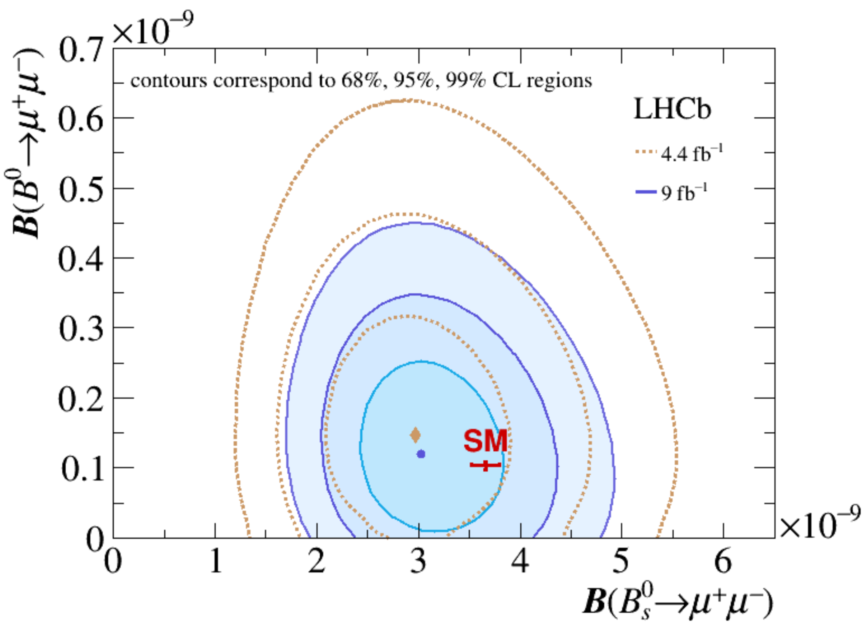

+

- CMS [JHEP 04 (2020) 188]
- ATLAS [JHEP 04 (2019) 098]

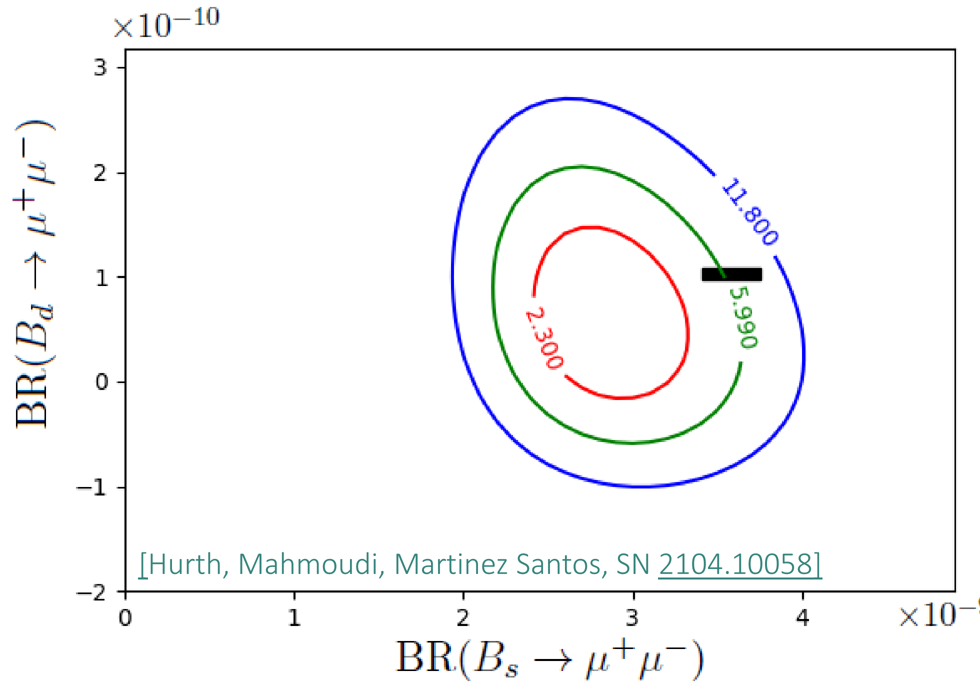

- Theory uncertainties $\lesssim 5\%$
- The SM prediction is near 2σ contour

Theoretical Framework

Theoretical framework: Weak Effective Hamiltonian

Separation between low and high energies using Operator Product Expansion

$$\mathcal{H}_{\text{eff}} = -\frac{4G_F}{\sqrt{2}} V_{tb} V_{ts}^* \left(\sum_{i=1\cdots 10,S,P} \left(C_i(\mu)\mathcal{O}_i(\mu) + C_i'(\mu)\mathcal{O}_i'(\mu) \right) \right)$$

4-quark operators

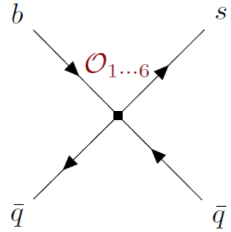

$\mathcal{O}_{1,2} \propto [\bar{s}\Gamma_\mu c]\,[\bar{c}\Gamma_\mu b]$

$\mathcal{O}_{3\cdots6} \propto [\bar{s}\Gamma_\mu b][\sum \bar{q}\Gamma^\mu q]$

electromagnetic dipole operator

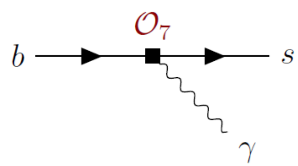

$\mathcal{O}_7 \propto [\bar{s}\sigma_{\mu\nu}P_R b]\, F^{\mu\nu}$

chromomagnetic dipole operator

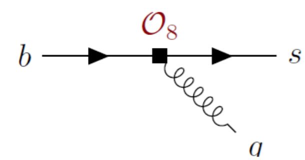

$\mathcal{O}_8 \propto [\bar{s}\sigma^{\mu\nu}T^a P_{R(L)} b]\, G^a_{\mu\nu}$

semileptonic operators

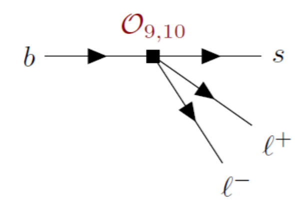

$\mathcal{O}_9^\ell \propto [\bar{s}\gamma_\mu P_L b][\bar{\ell}\gamma^\mu \ell]$

$\mathcal{O}_{10}^\ell \propto [\bar{s}\gamma_\mu P_L b][\bar{\ell}\gamma^\mu\gamma_5 \ell]$

In the SM: $C_7 \simeq -0.29$, $C_9 \simeq 4.20$, $C_{10} \simeq -4.16$

Additional operators: Chirality flipped (O_i'), (pseudo)scalar (O_S and O_P)

- Wilson coefficients $C_i \to C_i^{\text{SM}} + \delta C_i^{\text{NP}}$:
  perturbative, short-distance physics (q^2 independent), well-known in the SM
- Matrix elements of local operators:
  non-perturbative, long-distance physics (q^2 dependent), main source of uncertainty

Theoretical framework: Matrix elements for $B \to M\ell\ell$ ($M = K, K^*, \phi$)

Effective Hamiltonian has two parts: $\mathcal{H}_{\rm eff} = \mathcal{H}_{\rm eff}^{\rm sl} + \mathcal{H}_{\rm eff}^{\rm had}$

$$\mathcal{H}_{\rm eff}^{\rm sl} = -\frac{4G_F}{\sqrt{2}} V_{tb}V_{ts}^* \Big[\sum_{i=7,9,10,S,P} C_i^{(\prime)} \mathcal{O}_i^{(\prime)} \Big]$$

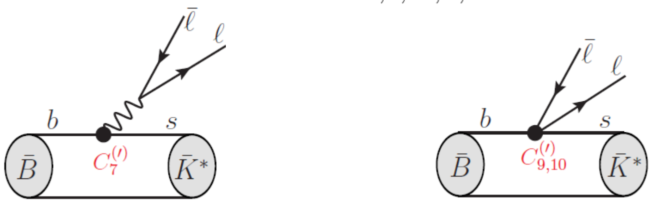

$$\langle M\ell\ell|\mathcal{H}_{\rm eff}^{\rm sl}|B\rangle \propto \mathcal{A}_V^\mu\, \bar{u}_\ell \gamma_\mu v_\ell + \mathcal{A}_A^\mu\, \bar{u}_\ell \gamma_\mu \gamma_5 v_\ell + \mathcal{A}_S\, \bar{u}_\ell v_\ell + \mathcal{A}_P\, \bar{u}_\ell \gamma_5 v_\ell$$

local contributions:

$$\mathcal{A}_V^\mu = -\frac{2im_b}{q^2} C_7 \langle M|\bar{s}\,\sigma^{\mu\nu} q_\nu\, P_R\, b|B\rangle + C_9 \langle M|\bar{s}\,\gamma^\mu\, P_L\, b|B\rangle$$

$$\mathcal{A}_A^\mu = C_{10} \langle M|\bar{s}\,\gamma^\mu\, P_L\, b|B\rangle$$

$$\mathcal{A}_{S,P} = C_{S,P} \langle M|\bar{s}\, P_R\, b|B\rangle$$

- 3 form factors for final state $M = K$
- 7 form factors for final state $M = K^*, \phi$

Determined by **Lattice QCD** (high q^2), **Light-Cone Sum Rules** (low q^2) and **combined fit of LCSR + Lattice** (low + high q^2)

Ball et al' '04; Khodjamirian et al. '10; HPQCD '13; Altmannshofer et al. '14; Bharucha et al. '15; MILC '15 ; Horgan et al. '15; Gubernari et al. '18

Theoretical framework: Matrix elements for $B \to M\ell\ell$ ($M = K, K^*, \phi$)

Effective Hamiltonian has two parts: $\mathcal{H}_{\text{eff}} = \mathcal{H}_{\text{eff}}^{\text{sl}} + \mathcal{H}_{\text{eff}}^{\text{had}}$

$$\mathcal{H}_{\text{eff}}^{\text{sl}} = -\frac{4G_F}{\sqrt{2}} V_{tb}V_{ts}^* \Big[\sum_{i=7,9,10,S,P} C_i^{(\prime)} \mathcal{O}_i^{(\prime)} \Big]$$

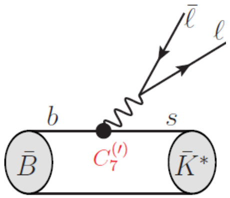

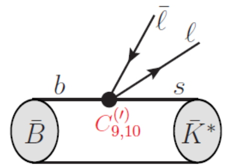

$$\langle M\ell\ell|\mathcal{H}_{\text{eff}}^{\text{sl}}|B\rangle \propto \mathcal{A}_V^\mu\, \bar{u}_\ell\gamma_\mu v_\ell + \mathcal{A}_A^\mu\, \bar{u}_\ell\gamma_\mu\gamma_5 v_\ell + \mathcal{A}_S\, \bar{u}_\ell v_\ell + \mathcal{A}_P\, \bar{u}_\ell\gamma_5 v_\ell$$

local contributions:

$$\mathcal{A}_V^\mu = -\frac{2im_b}{q^2} C_7 \langle M|\bar{s}\,\sigma^{\mu\nu} q_\nu\, P_R\, b|B\rangle + C_9\langle M|\bar{s}\,\gamma^\mu\, P_L\, b|B\rangle$$

$$\mathcal{A}_A^\mu = C_{10}\langle M|\bar{s}\,\gamma^\mu\, P_L\, b|B\rangle$$

$$\mathcal{A}_{S,P} = C_{S,P}\langle M|\bar{s}\, P_R\, b|B\rangle$$

- 3 form factors for final state $M = K$
- 7 form factors for final state $M = K^*, \phi$

Determined by **Lattice QCD** (high q^2), **Light-Cone Sum Rules** (low q^2) and **combined fit of LCSR + Lattice** (low + high q^2)

Ball et al' '04; Khodjamirian et al. '10; HPQCD '13; Altmannshofer et al. '14; Bharucha et al. '15; MILC '15 ; Horgan et al. '15; Gubernari et al. '18

$$\mathcal{H}_{\text{eff}}^{\text{had}} = -\frac{4G_F}{\sqrt{2}} V_{tb}V_{ts}^* \Big[\sum_{i=1\ldots6} C_i^{(\prime)} \mathcal{O}_i^{(\prime)} + C_8\mathcal{O}_8 \Big]$$

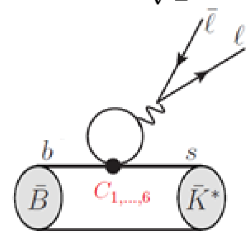

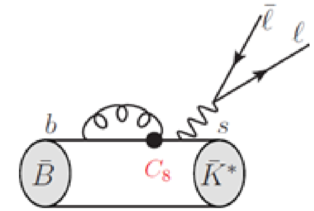

$$\langle M\ell\ell|\mathcal{H}_{\text{eff}}^{\text{had}}|B\rangle \propto \mathcal{N}^\mu \bar{u}_\ell\gamma_\mu v_\ell$$

non-local contributions:

$$\mathcal{H}^\mu = \frac{-16i\pi^2}{q^2} \sum_{i=1,\ldots,6,8} C_i \int dx^4 e^{iq\cdot x} \langle M|T\{j_{\text{em}}^\mu(x), O_i(0)\}|B\rangle$$

$$j_{\text{em}}^\mu = \sum_q Q_q\, \bar{q}\gamma^\mu q$$

Calculated for low q^2 at **LO in QCD factorization (QCDf)**

Beneke et al '01 and '04

higher powers not fully known ("guesstimated")

↪ recent progress using **analyticity + experimental data on $b \to sc\bar{c}$** show these corrections should be small

Bobeth et al. '17, Gubernari, et al. '20 and '22

$B \to K^* \ell\ell$ matrix elements:

local contributions: $\langle K^* | \mathcal{H}_{\rm eff}^{\rm sl} | B \rangle : \tilde{V}_\lambda(q^2), \tilde{T}_\lambda(q^2), \tilde{S}(q^2)$

non-local contributions: $\langle K^* | \mathcal{H}_{\rm eff}^{\rm had} | B \rangle : \mathcal{N}_\lambda \to \left[\text{LO from QCDf at low } q^2 + h_\lambda(q^2)\right]$

$B \to K^* \ell\ell$ helicity amplitudes:

$$H_V(\lambda) = -iN' \Big\{ (C_9 - C_9') \tilde{V}_\lambda(q^2) + \frac{m_B^2}{q^2} \Big[\frac{2m_b}{m_B} (C_7 - C_7{}') \tilde{T}_\lambda(q^2) - 16\pi^2 \mathcal{N}_\lambda(q^2) \Big] \Big\}$$

$$H_A(\lambda) = -iN' (C_{10} - C_{10}') \tilde{V}_\lambda(q^2)$$

$$H_P(\lambda) = iN' \Big\{ \frac{2m_\ell m_b}{q^2} (C_{10} - C_{10}') \tilde{S}(q^2) \Big\}$$

- Non-local contribution can mimic New Physics in $C_{7,9}$
  - To distinguish hadronic effects from NP in $C_{7,9}$ good control over hadronic contributions needed

Similar situation for $B_s \to \phi \ell\ell$ and $B \to K \ell\ell$

- In the LFUV ratios hadronic uncertainties cancel out
- For $\mathrm{BR}(B_s \to \mu^+\mu^-)$ only one hadronic parameter f_{B_s}

"clean observables"

Global Fit

How to make sense of data?

Many $b \to s\ell^+\ell^-$ observables

- $R_K, R_{K^*}, R_{K_S}, R_{K^{*+}}$
- BR$\left(B_{s,d} \to \mu^+\mu^-\right)$
- BR$(B_s \to e^+e^-)$
- BR$(B \to X_s\, \mu^+\mu^-)$
- BR$(B \to X_s\, e^+e^-)$
- BR$(B \to K^* e^+e^-)$: BR, ang. Obs.
- $B_s \to \phi\, \mu^+\mu^-$: BR, ang. obs.
- $B^{0(+)} \to K^{0(+)}\mu^+\mu^-$: BR, ang. obs.
- $B^{(+)} \to K^{*(+)}\mu^+\mu^-$: BR, ang. obs.
- $\Lambda_b \to \Lambda\, \mu^+\mu^-$: BR, ang. obs.

183 observable ⇒ Global fits

Minimization of χ^2, scanning over the values of δC_i

$$\chi^2 = \left(\vec{O}^{\rm th}(\delta C_i) - \vec{O}^{\rm exp}\right) \cdot \left(\Sigma_{\rm th} + \Sigma_{\rm exp}\right)^{-1} \cdot \left(\vec{O}^{\rm th}(\delta C_i) - \vec{O}^{\rm exp}\right)$$

$\left(\Sigma_{\rm th} + \Sigma_{\rm exp}\right)^{-1}$: the inverse covariance matrix

Theoretical uncertainties and correlations

- Monte Carlo analysis
- Variation of the input parameters: masses, scales, CKM, decay constants, form factors, ...
- Parameterization of uncertainties due to power corrections:

Leading Order QCDf of non-factorisable piece $\times \left(1 + a_k \exp(i\phi_k) + b_k \frac{q^2}{6\ \text{GeV}^2} \exp(i\theta_k)\right)$ with a_k 10 to 60%, $b_k \sim 2.5 a_k$

Computations performed using **SuperIso** public program

NP fit with a single operator

Comparison of one-operator NP fits:

Only LFUV ratios and $B_{s,d} \to \ell^+\ell^-$ **2021 data** $(\chi^2_{\rm SM} = 34.25)$			
	b.f. value	$\chi^2_{\rm min}$	$\mathrm{Pull}_{\rm SM}$
δC_9	-2.00 ± 5.00	34.1	0.4σ
δC_9^e	0.83 ± 0.21	14.5	4.4σ
δC_9^μ	-0.80 ± 0.21	15.4	4.3σ
δC_{10}	0.43 ± 0.24	30.6	1.9σ
δC_{10}^e	-0.81 ± 0.19	12.3	4.7σ
δC_{10}^μ	0.66 ± 0.15	10.3	4.9σ
$\delta C_{\rm LL}^e$	0.43 ± 0.11	13.3	4.6σ
$\delta C_{\rm LL}^\mu$	-0.39 ± 0.08	10.1	4.9σ

↓
Clean observables

δC_{LL} basis corresponds to $\delta C_9 = -\delta C_{10}$

NP fit with a single operator

Comparison of one-operator NP fits:

Only LFUV ratios and $B_{s,d} \to \ell^+\ell^-$ **2021 data** $(\chi^2_{\rm SM} = 34.25)$			
	b.f. value	$\chi^2_{\rm min}$	$\mathrm{Pull}_{\rm SM}$
δC_9	-2.00 ± 5.00	34.1	0.4σ
δC_9^e	0.83 ± 0.21	14.5	4.4σ
δC_9^μ	-0.80 ± 0.21	15.4	4.3σ
δC_{10}	0.43 ± 0.24	30.6	1.9σ
δC_{10}^e	-0.81 ± 0.19	12.3	4.7σ
δC_{10}^μ	0.66 ± 0.15	10.3	4.9σ
$\delta C_{\rm LL}^e$	0.43 ± 0.11	13.3	4.6σ
$\delta C_{\rm LL}^\mu$	-0.39 ± 0.08	10.1	4.9σ

↓

Clean observables

All obs. except LFUV ratios and $B_{s,d} \to \ell^+\ell^-$ **2021 data** $(\chi^2_{\rm SM} = 221.8)$			
	b.f. value	$\chi^2_{\rm min}$	$\mathrm{Pull}_{\rm SM}$
δC_9	-0.95 ± 0.13	185.1	6.1σ
δC_9^e	0.70 ± 0.60	220.5	1.1σ
δC_9^μ	-0.96 ± 0.13	182.8	6.2σ
δC_{10}	0.29 ± 0.21	219.8	1.4σ
δC_{10}^e	-0.60 ± 0.50	220.6	1.1σ
δC_{10}^μ	0.35 ± 0.20	218.7	1.8σ
$\delta C_{\rm LL}^e$	0.34 ± 0.29	220.6	1.1σ
$\delta C_{\rm LL}^\mu$	-0.64 ± 0.13	195.0	5.2σ

δC_{LL} basis corresponds to $\delta C_9 = -\delta C_{10}$

- Compatible NP scenarios between different sets

NP fit with a single operator

Comparison of one-operator NP fits:

Only LFUV ratios and $B_{s,d} \to \ell^+\ell^-$ **2021 data** ($\chi^2_{\rm SM} = 34.25$)	b.f. value	$\chi^2_{\rm min}$	$\mathrm{Pull_{SM}}$
δC_9	-2.00 ± 5.00	34.1	0.4σ
δC_9^e	0.83 ± 0.21	14.5	4.4σ
δC_9^μ	-0.80 ± 0.21	15.4	4.3σ
δC_{10}	0.43 ± 0.24	30.6	1.9σ
δC_{10}^e	-0.81 ± 0.19	12.3	4.7σ
δC_{10}^μ	0.66 ± 0.15	10.3	4.9σ
$\delta C_{\rm LL}^e$	0.43 ± 0.11	13.3	4.6σ
$\delta C_{\rm LL}^\mu$	-0.39 ± 0.08	10.1	4.9σ

All obs. except LFUV ratios and $B_{s,d} \to \ell^+\ell^-$ **2021 data** ($\chi^2_{\rm SM} = 221.8$)	b.f. value	$\chi^2_{\rm min}$	$\mathrm{Pull_{SM}}$
δC_9	-0.95 ± 0.13	185.1	6.1σ
δC_9^e	0.70 ± 0.60	220.5	1.1σ
δC_9^μ	-0.96 ± 0.13	182.8	6.2σ
δC_{10}	0.29 ± 0.21	219.8	1.4σ
δC_{10}^e	-0.60 ± 0.50	220.6	1.1σ
δC_{10}^μ	0.35 ± 0.20	218.7	1.8σ
$\delta C_{\rm LL}^e$	0.34 ± 0.29	220.6	1.1σ
$\delta C_{\rm LL}^\mu$	-0.64 ± 0.13	195.0	5.2σ

All observables **2021 data** ($\chi^2_{\rm SM} = 253.3$)	b.f. value	$\chi^2_{\rm min}$	$\mathrm{Pull_{SM}}$
δC_9	-0.93 ± 0.13	218.4	5.9σ
δC_9^e	0.82 ± 0.19	232.3	4.6σ
δC_9^μ	-0.90 ± 0.11	197.7	7.5σ
δC_{10}	0.27 ± 0.17	250.5	1.7σ
δC_{10}^e	-0.78 ± 0.18	230.4	4.8σ
δC_{10}^μ	0.54 ± 0.12	231.5	4.7σ
$\delta C_{\rm LL}^e$	0.42 ± 0.10	231.2	4.7σ
$\delta C_{\rm LL}^\mu$	-0.46 ± 0.07	208.2	6.7σ

↓ Clean observables

↓ ↓ Depends on the assumptions on the non-factorisable power corrections

δC_{LL} basis corresponds to $\delta C_9 = -\delta C_{10}$

- Compatible NP scenarios between different sets
- Hierarchy of preferred NP scenarios have remained the same with updated data compared to 2019 (δC_9^μ followed by δC_{LL}^μ)
- Significance increased by more than 2σ in the preferred scenarios compared to 2019

NP fit with two operators; clean observables

Fit to clean observables $R_K, R_{K^*}, B_s \to \mu^+\mu^-$

Coloured regions: 1σ range (th + exp uncertainties added in quadrature) with the experimental central value

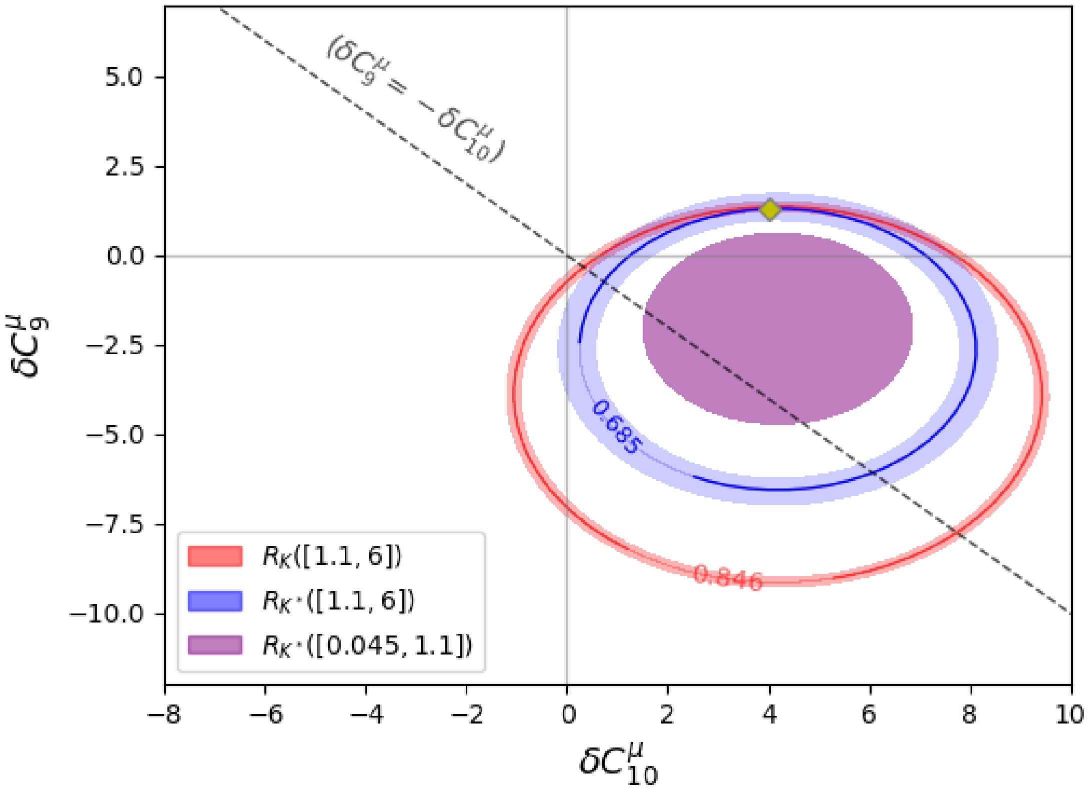

Yellow diamond ◇ : best fit point of $(\delta C_9^\mu, \delta C_{10}^\mu)$ fit to $R_K + R_{K^*}$

Fit to clean observables $R_K, R_{K^*}, B_s \to \mu^+\mu^-$

Coloured regions: 1σ range (th + exp uncertainties added in quadrature) with the experimental central value

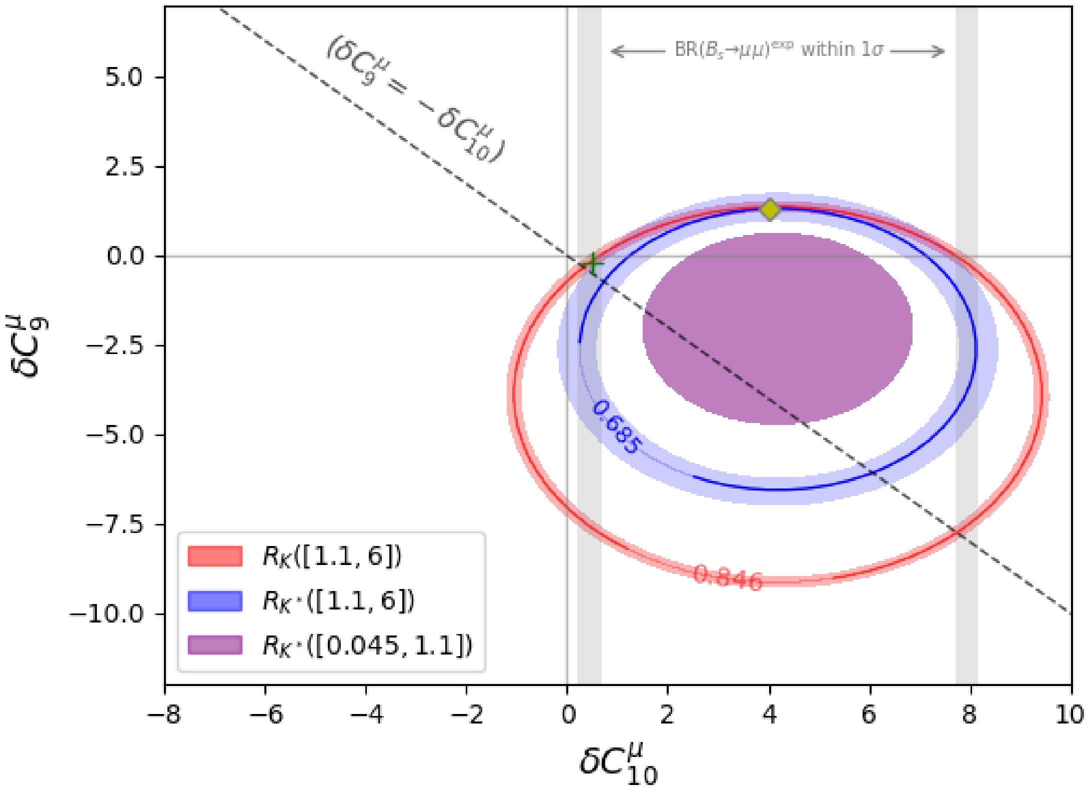

Yellow diamond ◇ : best fit point of $(\delta C_9^\mu, \delta C_{10}^\mu)$ fit to $R_K + R_{K^*}$

Green cross +: best fit point of $(\delta C_9^\mu, \delta C_{10}^\mu)$ fit to $R_K + R_{K^*} + B_s \to \mu^+\mu^-$

NP fit with two operators; clean observables

Fit to clean observables $R_K, R_{K^*}, B_s \to \mu^+\mu^-$

Coloured regions: 1σ range (th + exp uncertainties added in quadrature) with the experimental central value

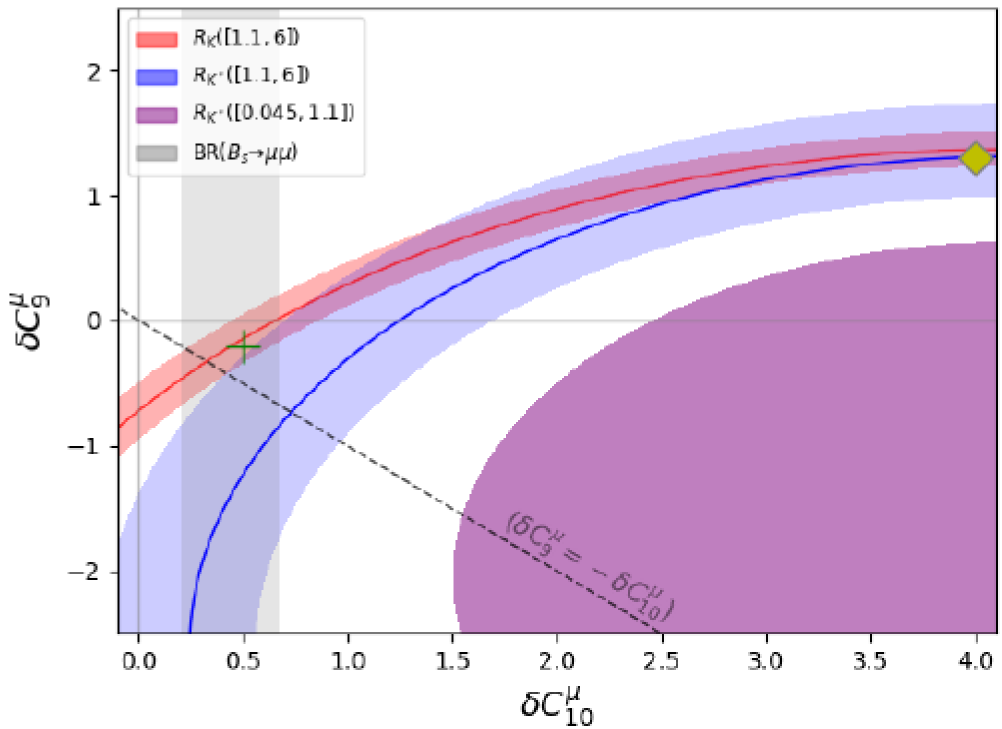

Yellow diamond : best fit point of $(\delta C_9^\mu, \delta C_{10}^\mu)$ fit to $R_K + R_{K^*}$

Green cross +: best fit point of $(\delta C_9^\mu, \delta C_{10}^\mu)$ fit to $R_K + R_{K^*} + B_s \to \mu^+\mu^-$

NP fit with two operators; all observables

Considering all the relevant data on $b \to s$ transitions (183 observables)

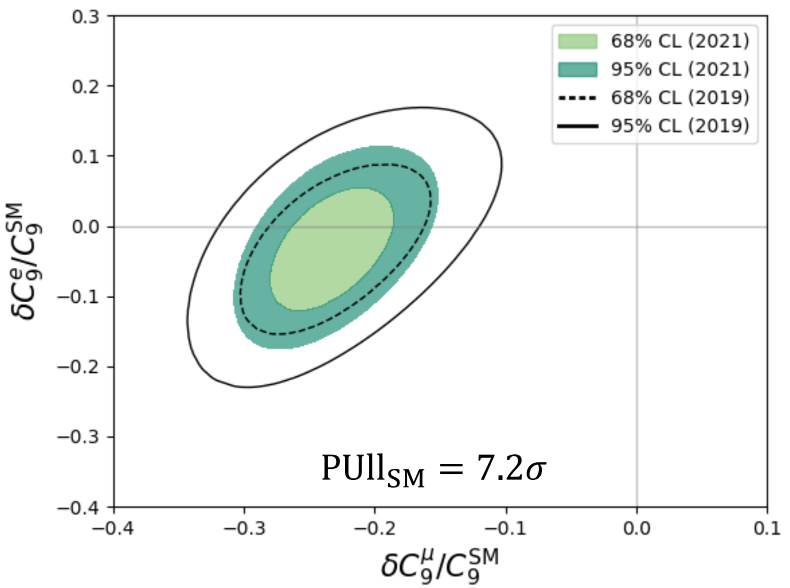

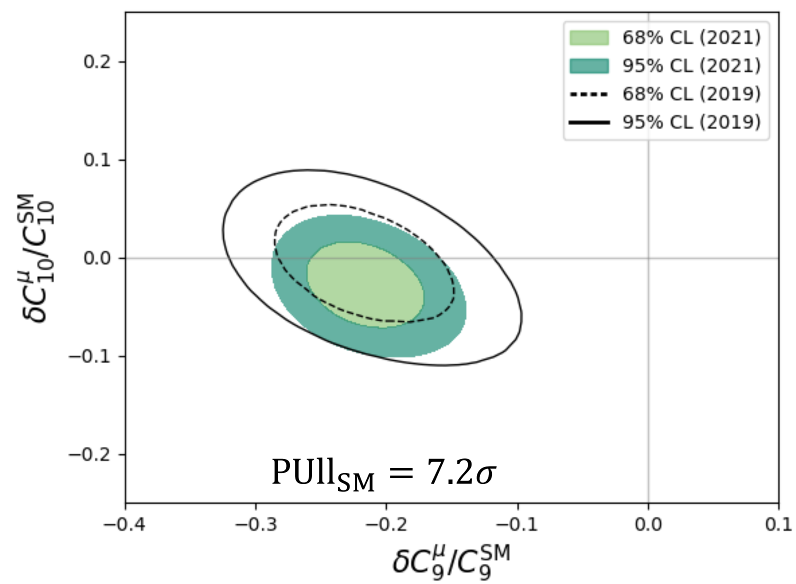

Similar fits by other groups:

Altmannshofer et al. arXiv: 2103.13370, Algueró et al. arXiv:2104.08921, Ciuchini et al. arXiv:2011.01212, Datta et al. 1903.10086, Geng et al. arXiv:2103.12738, Kowalska et al., arXiv:1903.10932

Multi-dimensional fit

Considering only one or two Wilson coefficients may not give the full picture!

All relevant Wilson coefficients:

$$C_7, C_8, C_9^\ell, C_{10}^\ell, C_S^\ell, C_P^\ell + \text{primed coefficients} \longrightarrow 20 \text{ degrees of freedom}$$

- Considering the most general NP description, look-elsewhere effect is avoided

All observables with $\chi^2_{\rm SM} = 253.3$			
2021 data ($\chi^2_{\rm min} = 179.2$; $\text{Pull}_{\rm SM} = 5.5(5.5)\sigma$)			
δC_7		δC_8	
0.06 ± 0.03		-0.80 ± 0.40	
$\delta C_7'$		$\delta C_8'$	
-0.01 ± 0.01		-0.30 ± 1.30	
δC_9^μ	δC_9^e	δC_{10}^μ	δC_{10}^e
-1.15 ± 0.18	-6.60 ± 1.60	0.21 ± 0.20	degenerate w/ $C_{10}^{\prime e}$
$\delta C_9^{\prime\mu}$	$\delta C_9^{\prime e}$	$\delta C_{10}^{\prime\mu}$	$\delta C_{10}^{\prime e}$
0.05 ± 0.31	1.40 ± 2.10	-0.04 ± 0.19	degenerate w/ C_{10}^e
$C_{Q_1}^\mu$	$C_{Q_1}^e$	$C_{Q_2}^\mu$	$C_{Q_2}^e$
0.07 ± 0.06	-1.60 ± 1.60	-0.11 ± 0.14	-4.00 ± 1.2
$C_{Q_1}^{\prime\mu}$	$C_{Q_1}^{\prime e}$	$C_{Q_2}^{\prime\mu}$	$C_{Q_2}^{\prime e}$
-0.07 ± 0.06	-1.70 ± 1.30	-0.21 ± 0.15	-4.10 ± 0.8

- Insensitive Wilson coefficients and flat directions eliminated via likelihood profiles and corr. matrices

↪ Effective dof = (19) giving 5.5σ significance

Comparison of different fitting groups

Comparison between fits of different groups

Joint theory presentation at Flavour Anomaly Workshop 2021 [B. Capdevila, M. Fedele, SN, Stangl]

- ACDMN (M. Algueró, B. Capdevila, S. Descotes-Genon, J. Matias, M. Novoa-Brunet) [arXiv:2104.08921]
- AS (W. Altmannshofer, P. Stangl) [arXiv:2103.13370]
- CFFPSV (M. Ciuchini, M. Fedele, E. Franco, A. Paul, L. Silvestrini, M. Valli) [arXiv:2011.01212]
- HMMN (T. Hurth, F. Mahmoudi, D. Martínez-Santos, S. Neshatpour) [arXiv:2104.10058]

- different assumptions about non-local matrix elements, form factor inputs, experimental inputs, etc. and different statistical frameworks

One-dimensional fits:

All observables

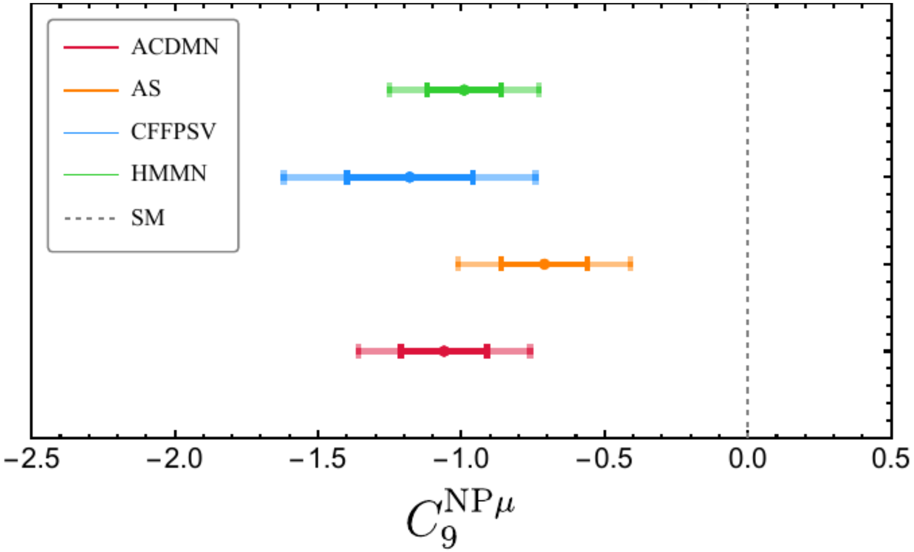

All observables

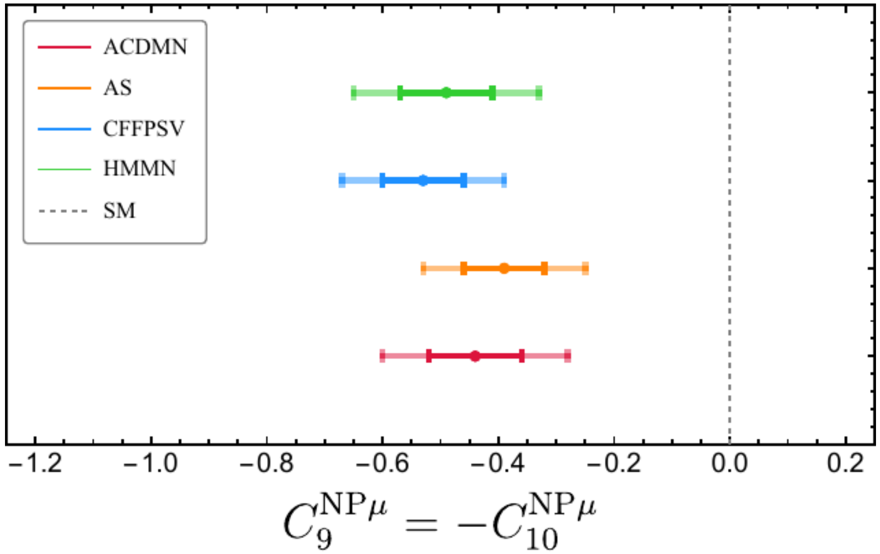

Joint theory presentation at Flavour Anomaly Workshop 2021 [B. Capdevila, M. Fedele, SN, Stangl]

- ACDMN (M. Algueró, B. Capdevila, S. Descotes-Genon, J. Matias, M. Novoa-Brunet) [arXiv:2104.08921]
- AS (W. Altmannshofer, P. Stangl) [arXiv:2103.13370]
- CFFPSV (M. Ciuchini, M. Fedele, E. Franco, A. Paul, L. Silvestrini, M. Valli) [arXiv:2011.01212]
- HMMN (T. Hurth, F. Mahmoudi, D. Martínez-Santos, S. Neshatpour) [arXiv:2104.10058]

❑ different assumptions about non-local matrix elements, form factor inputs, experimental inputs, etc. and different statistical frameworks

Two-dimensional fits:

All observables

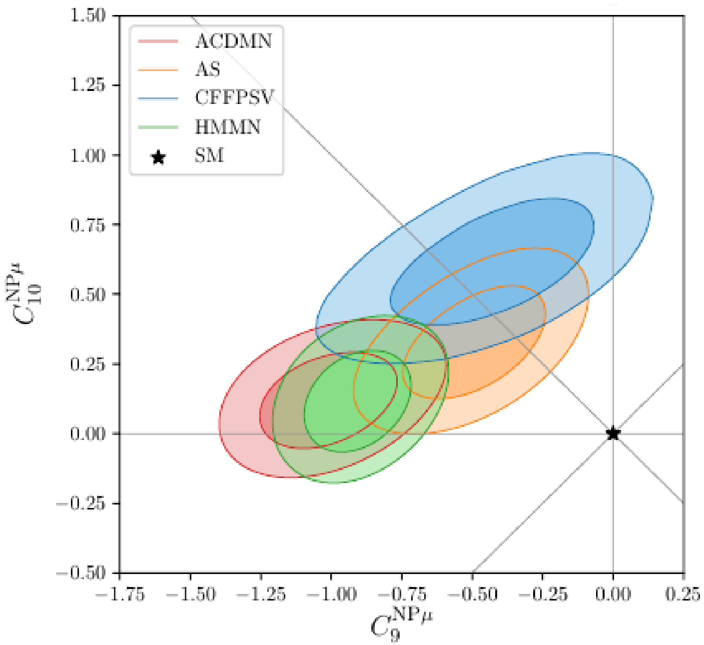

Clean observables

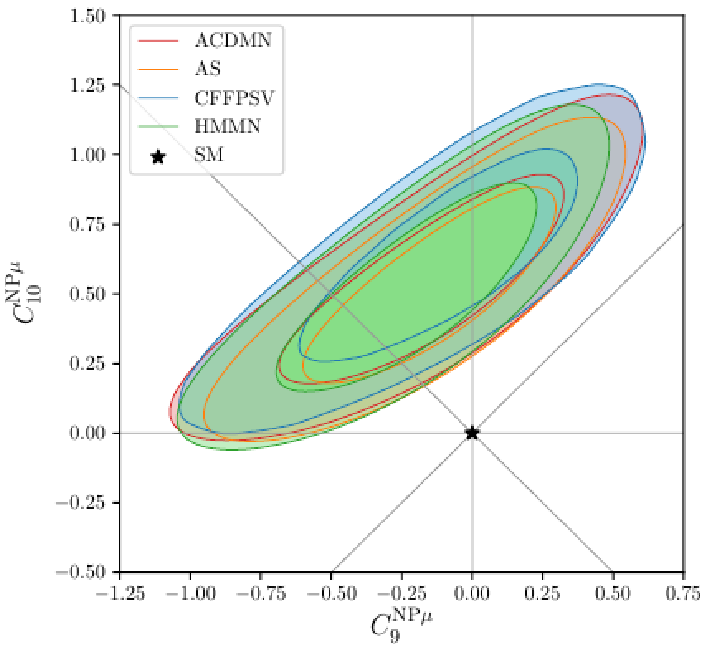

Prospect of clean observables

Evolution of the tension between the SM and the experimental values

Assuming the best fit value of δC_9^μ (left) and δC_{10}^μ (right)

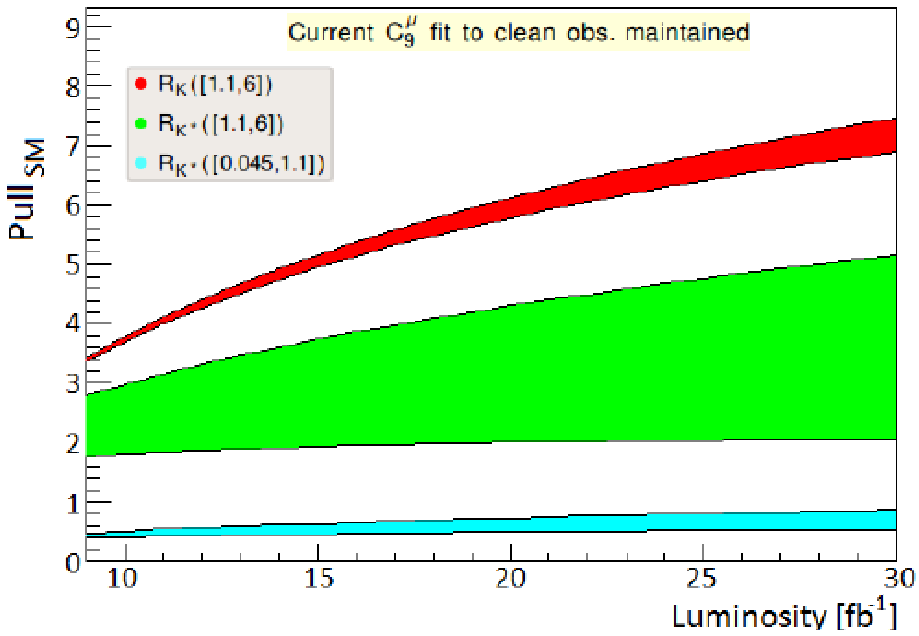

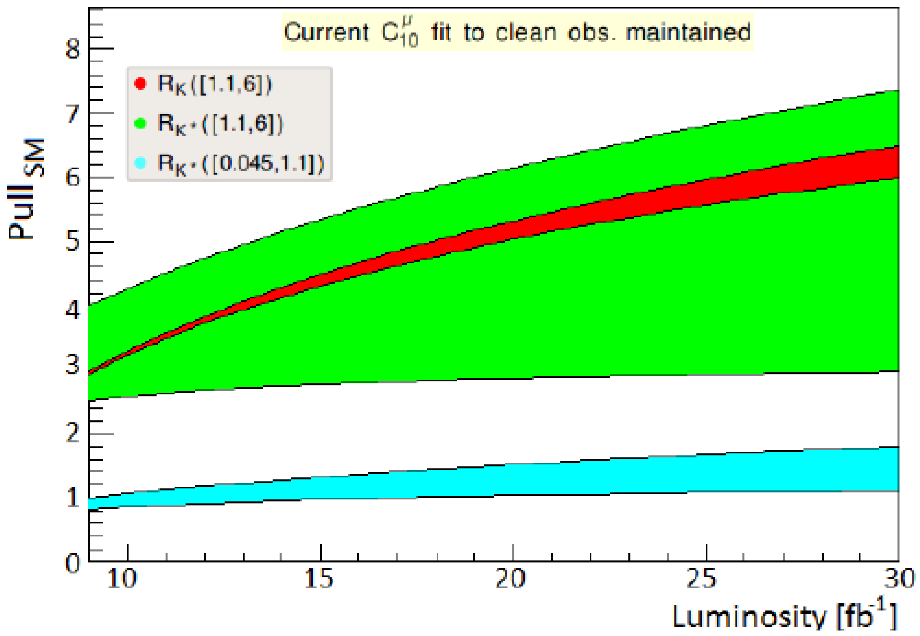

Upper limit: assuming ultimate systematic uncertainty (1% for ratios & 4% for $B_s \to \mu^+\mu^-$)

Lower limit: assuming current systematic uncertainties do not improve

- For the δC_9^μ case, R_K can individually reach 5σ at $\sim 16\ \mathrm{fb}^{-1}$

Projections: one operator fit to clean observables

Projections of Pull_{SM} for 1-dimensional fit to δC_9^μ or δC_{10}^μ or δC_{LL}^μ

- using only the clean observables R_K, R_{K^*} and $B_s \to \mu^+\mu^-$
- assuming LHCb upgrade scenarios with 18, 50 and 300 fb^{-1} collected luminosity

Pull_{SM} with $R_{K^{(*)}}$ and $\text{BR}(B_s \to \mu^+\mu^-)$ prospects			
LHCb lum.	18 fb^{-1}	50 fb^{-1}	300 fb^{-1}
δC_9^μ	6.5σ	14.7σ	21.9σ
δC_{10}^μ	7.1σ	16.6σ	25.1σ
δC_{LL}^μ	7.5σ	17.7σ	26.6σ

- For all three scenarios NP significance will be larger than 6σ already with 18 fb^{-1}

Projections: two operator fit to clean observables

Projections of 2-dimensional fits

- using only the clean observables R_K, R_{K^*} and $B_s \to \mu^+\mu^-$
- assuming LHCb upgrade scenarios with 18, 50 and 300 fb^{-1} collected luminosity

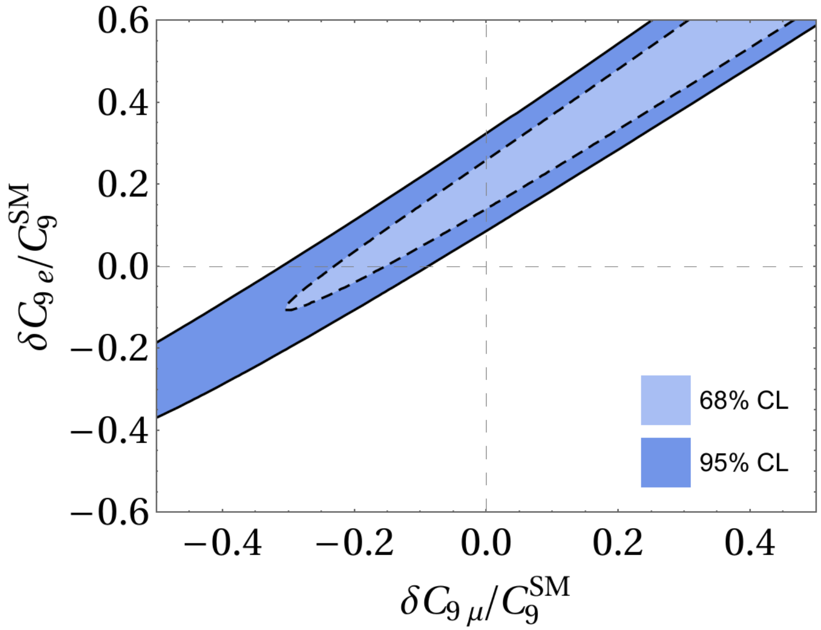

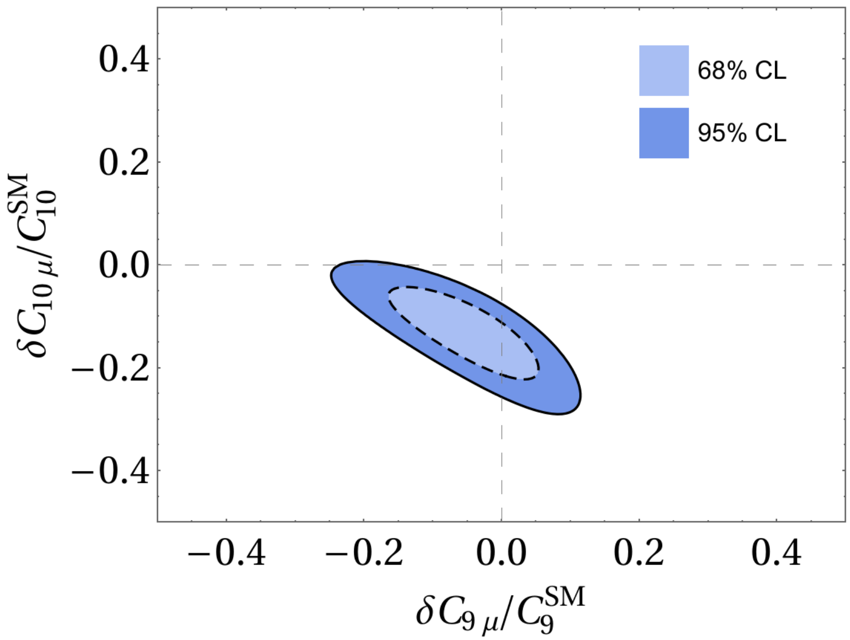

Current data

Projections of 2-dimensional fits

- using only the clean observables R_K, R_{K^*} and $B_s \to \mu^+\mu^-$
- assuming LHCb upgrade scenarios with 18, 50 and 300 fb^{-1} collected luminosity

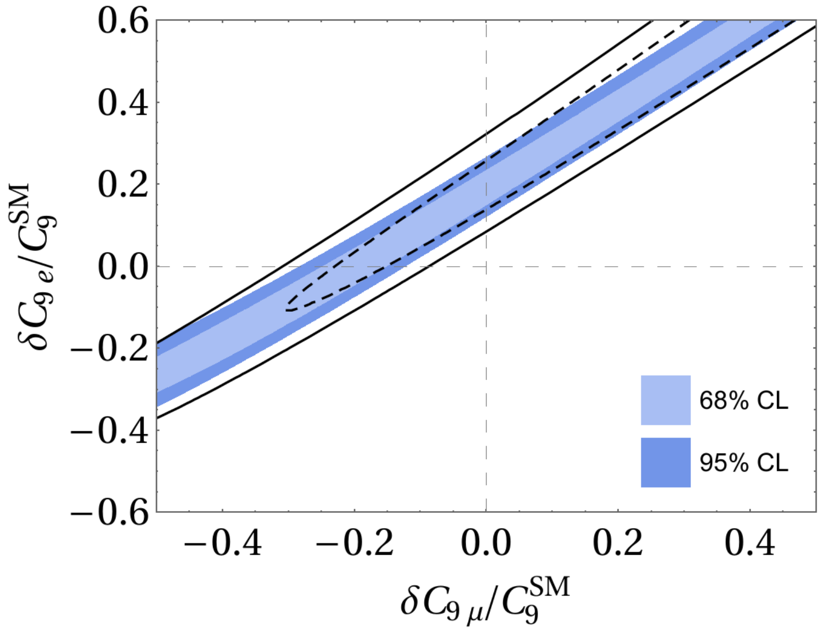

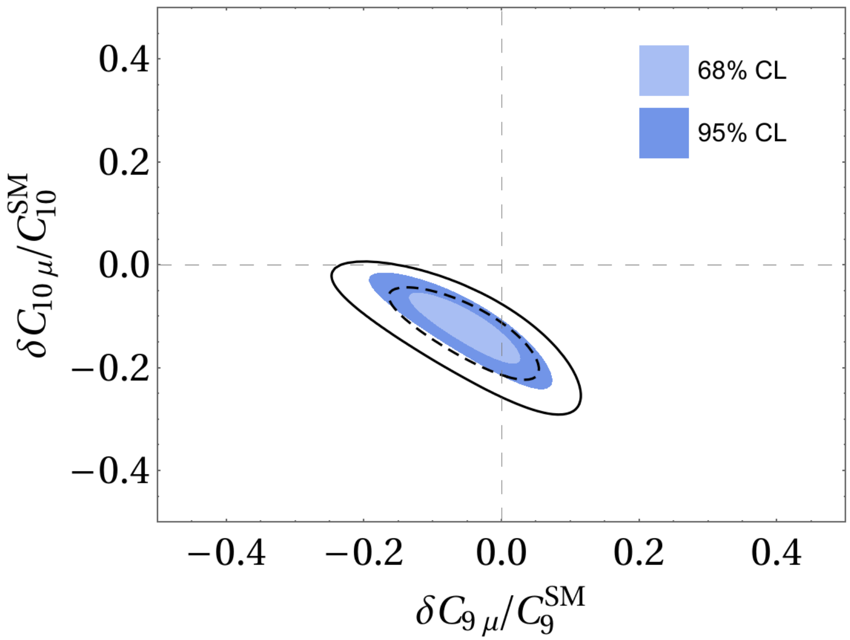

Projections for 18 fb^{-1}

Projections: two operator fit to clean observables

Projections of 2-dimensional fits

- using only the clean observables R_K, R_{K^*} and $B_s \to \mu^+\mu^-$
- assuming LHCb upgrade scenarios with 18, 50 and 300 fb^{-1} collected luminosity

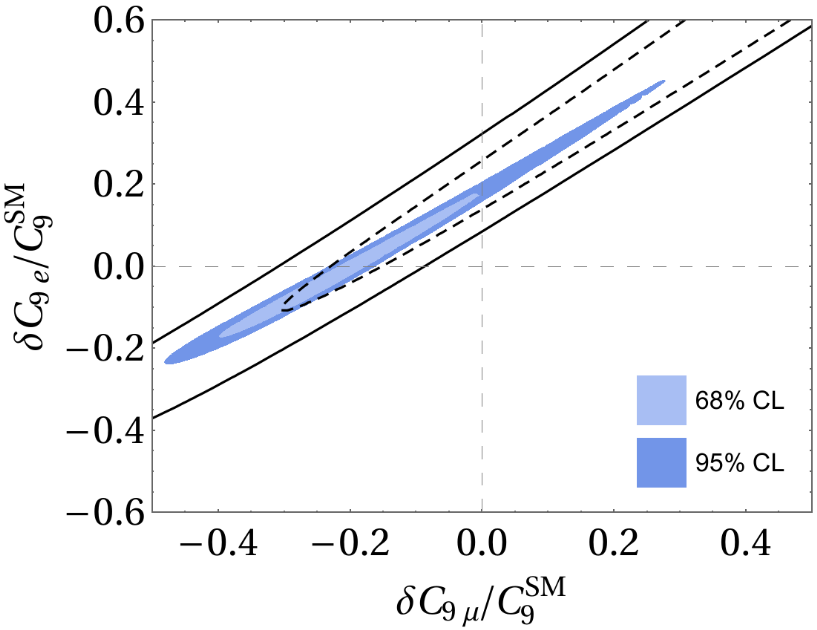

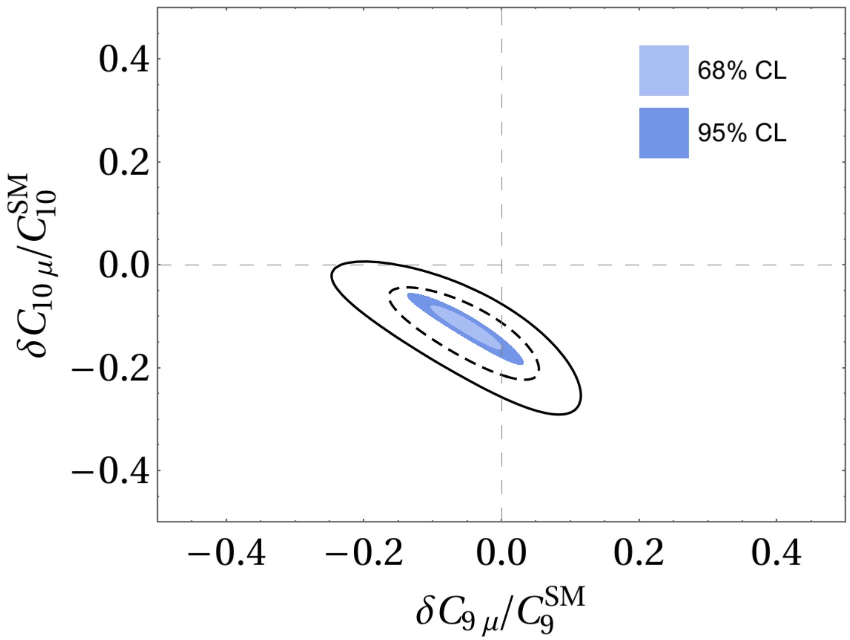

Projections for 50 fb^{-1}

Projections: two operator fit to clean observables

Projections of 2-dimensional fits

- using only the clean observables R_K, R_{K^*} and $B_s \to \mu^+\mu^-$
- assuming LHCb upgrade scenarios with 18, 50 and 300 fb^{-1} collected luminosity

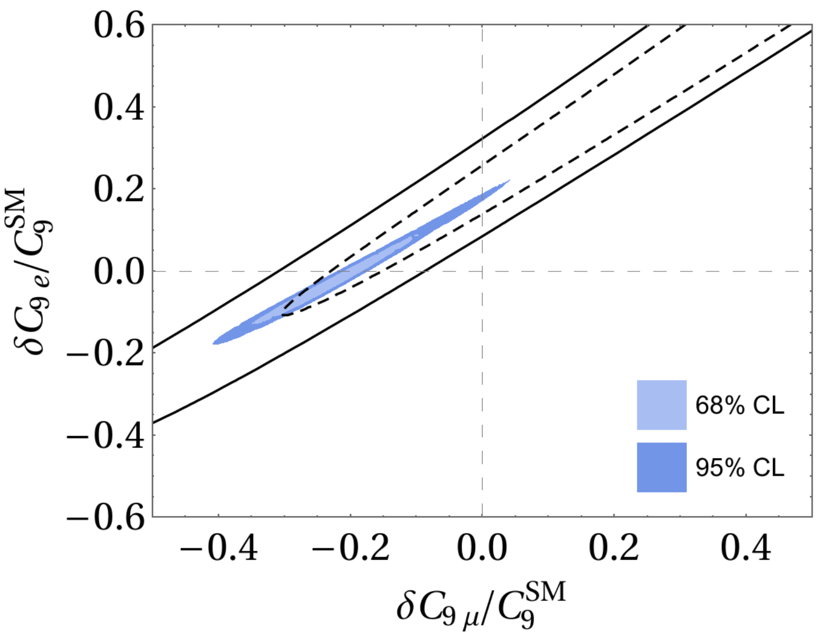

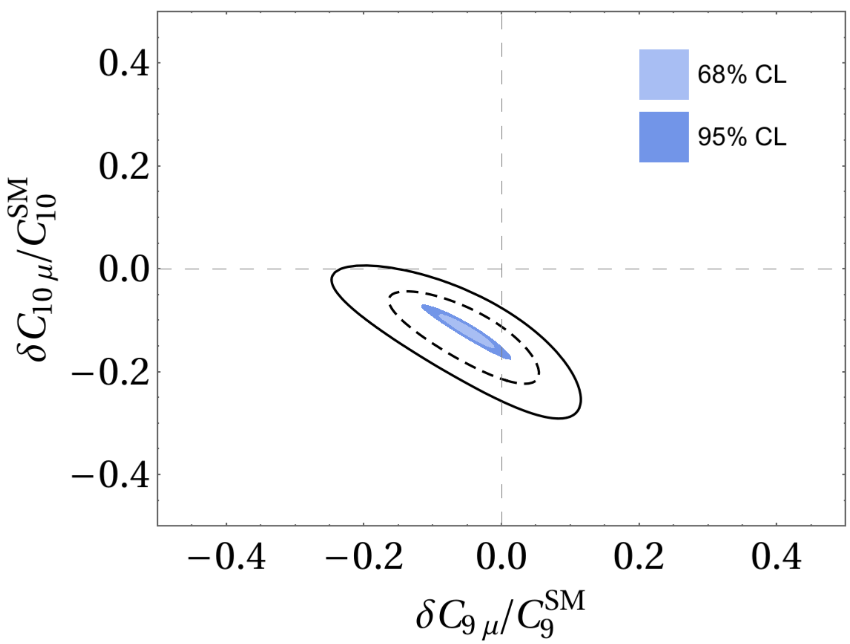

Projections for 300 fb^{-1}

Conclusions

- Experimental measurements show persistent tensions with the SM predictions in $b \to s\ell\ell$ transitions which can be consistently explained by New Physics

- The most preferred NP fits are δC_9 and/or δC_{10}

- Main source of theory uncertainty in global fit due to non-local hadronic contributions

- Fit to clean observables and the rest of the $b \to s\ell\ell$ observables point towards compatible NP scenarios

- Different fits with different setups, inputs and statistical frameworks show remarkable agreement

- Using clean observables, future data can pin down δC_9, δC_{10}, δC_{LL} assuming that's where new physics is

Conclusions

- Experimental measurements show persistent tensions with the SM predictions in $b \to s\ell\ell$ transitions which can be consistently explained by New Physics

- The most preferred NP fits are δC_9 and/or δC_{10}

- Main source of theory uncertainty in global fit due to non-local hadronic contributions

- Fit to clean observables and the rest of the $b \to s\ell\ell$ observables point towards compatible NP scenarios

- Different fits with different setups, inputs and statistical frameworks show remarkable agreement

- Using clean observables, future data can pin down δC_9, δC_{10}, δC_{LL} assuming that's where new physics is

Thank you!

Backup

Hadronic fit for $B \to K^* \mu\mu$

Projections: further ratios

Other clean $R_{\mu/e}$ to differentiate between preferred NP scenario

	Predictions assuming 50 fb^{-1} luminosity					
Obs.	C_9^μ	C_9^e	C_{10}^μ	C_{10}^e	C_{LL}^μ	C_{LL}^e
$R_{F_L}^{[1.1,6.0]}$	$[0.922, 0.932]$	$[0.941, 0.944]$	$[0.995, 0.998]$	$[0.996, 0.997]$	$[0.961, 0.964]$	$[1.006, 1.010]$
$R_{A_{FB}}^{[1.1,6.0]}$	$[4.791, 5.520]$	$[-0.416, -0.358]$	$[0.938, 0.939]$	$[0.963, 0.970]$	$[2.822, 3.089]$	$[0.279, 0.307]$
$R_{S_3}^{[1.1,6.0]}$	$[0.922, 0.931]$	$[0.914, 0.922]$	$[0.832, 0.852]$	$[0.858, 0.870]$	$[0.853, 0.870]$	$[1.027, 1.032]$
$R_{S_5}^{[1.1,6.0]}$	$[0.453, 0.543]$	$[0.723, 0.742]$	$[1.014, 1.014]$	$[1.040, 1.048]$	$[0.773, 0.801]$	$[1.298, 1.361]$
$R_{F_L}^{[15,19]}$	$[0.998, 0.999]$	$[0.998, 0.998]$	$[0.998, 0.998]$	$[0.998, 0.998]$	$[0.998, 0.998]$	$[0.998, 0.998]$
$R_{A_{FB}}^{[15,19]}$	$[0.929, 0.944]$	$[0.988, 0.989]$	$[1.009, 1.010]$	$[1.036, 1.042]$	$[0.996, 0.996]$	$[1.023, 1.028]$
$R_{S_3}^{[15,19]}$	$[0.998, 0.998]$	$[0.998, 0.998]$	$[0.999, 0.999]$	$[0.999, 0.999]$	$[0.999, 0.999]$	$[0.998, 0.998]$
$R_{S_5}^{[15,19]}$	$[0.929, 0.944]$	$[0.988, 0.989]$	$[1.009, 1.010]$	$[1.036, 1.042]$	$[0.996, 0.996]$	$[1.023, 1.028]$
$R_{K^*}^{[15,19]}$	$[0.825, 0.847]$	$[0.815, 0.835]$	$[0.828, 0.846]$	$[0.799, 0.820]$	$[0.804, 0.825]$	$[1.093, 1.107]$
$R_{K}^{[15,19]}$	$[0.823, 0.847]$	$[0.819, 0.838]$	$[0.854, 0.870]$	$[0.825, 0.844]$	$[0.820, 0.839]$	$[1.098, 1.113]$
$R_{\phi}^{[1.1,6.0]}$	$[0.862, 0.879]$	$[0.841, 0.858]$	$[0.824, 0.843]$	$[0.795, 0.816]$	$[0.819, 0.839]$	$[1.070, 1.080]$
$R_{\phi}^{[15,19]}$	$[0.825, 0.847]$	$[0.815, 0.835]$	$[0.826, 0.845]$	$[0.797, 0.819]$	$[0.803, 0.824]$	$[1.093, 1.107]$

Electrons are more SM-like than muons

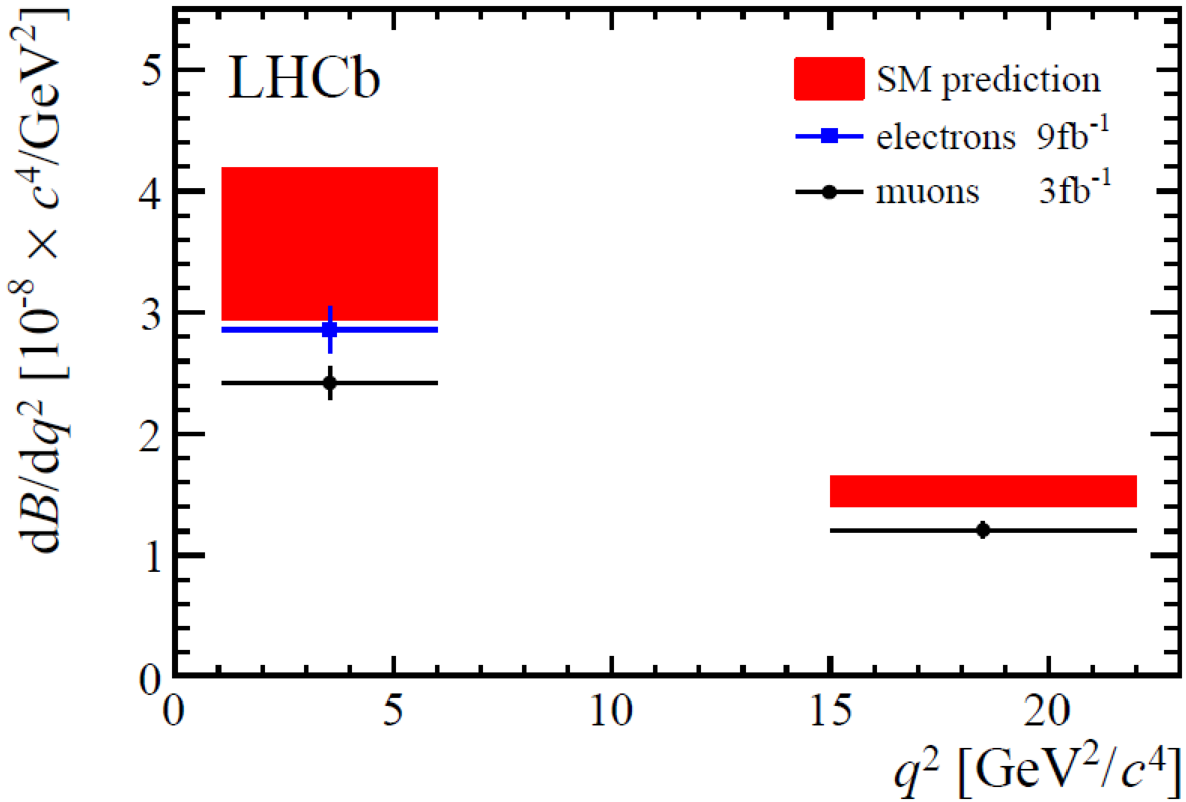

One operator fit

Fit to clean observables $R_K, R_{K^{(*)}}, B_s \to \mu^+\mu^-$ and the rest of the $b \to s\ell\ell$ obs.

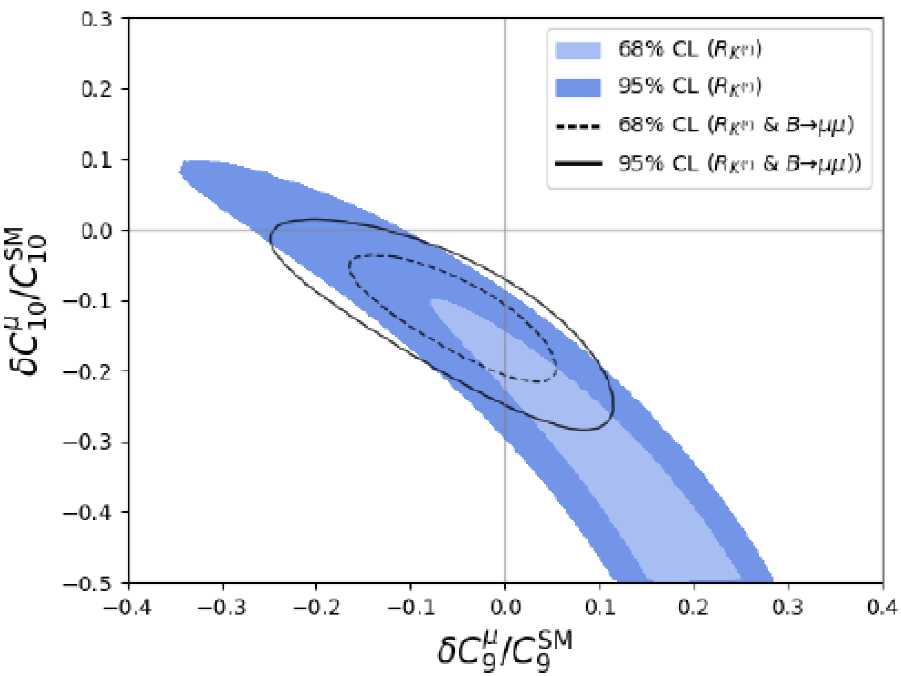

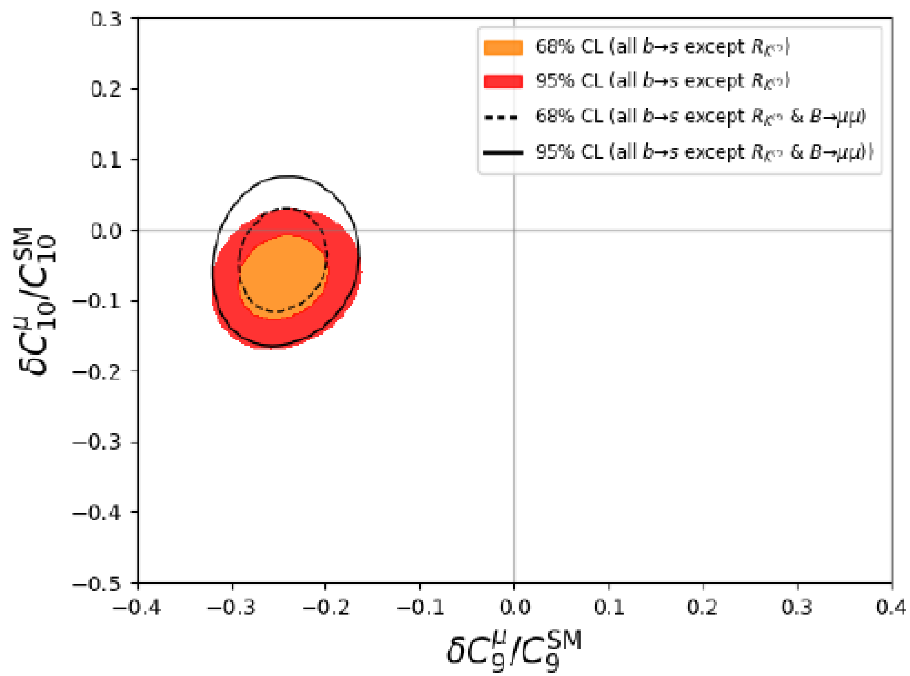

Depends on the assumptions on the non-factorisable power corrections

Global analysis of $b \to s$ transitions: multi-dimensional fit

Multi-dimensional fit: $C_7, C_8, C_9^\ell, C_{10}^\ell, C_S^\ell, C_P^\ell$ + primed coefficients

Set of WC	param.	$\chi^2_{\rm min}$	$\mathrm{Pull}_{\rm SM}$	Improvement
SM	0	225.8	-	-
C_9^μ	1	168.6	7.6σ	7.6σ
C_9^μ, C_{10}^μ	2	167.5	7.3σ	1.0σ
$C_7, C_8, C_9^{(e,\mu)}, C_{10}^{(e,\mu)}$	6	158.0	7.1σ	2.0σ
All non-primed WC	10	157.2	6.5σ	0.1σ
All WC (incl. primed)	20 (19)	151.6	$5.5\,(5.6)\sigma$	$0.2\,(0.3)\sigma$

Hadronic uncertainties

1. *Different assumptions on the form factor uncertainties*

> Filled area: global fit with normal form factor error
> Bharucha, Straub, Zwicky: 1503.05534
> Solid contour: removing form factor error correlations
> Dashed contour: 2 x form factor errors
> Dotted contour: 4 x form factor errors

- Only when assuming $4 \times$ form factor errors tensions goes below 2σ

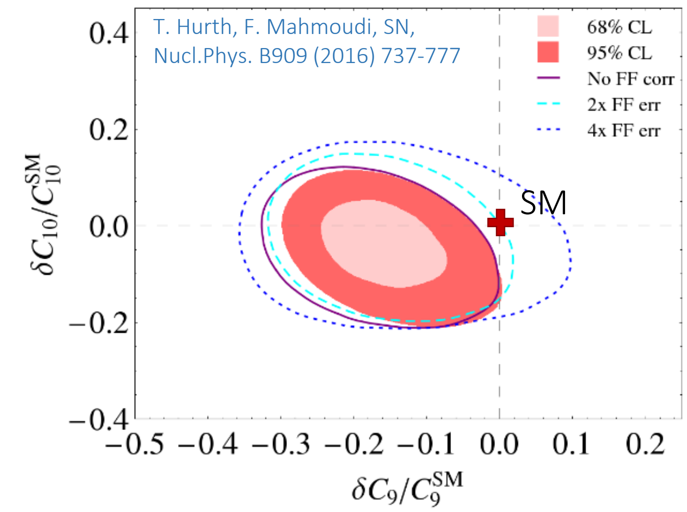

2. *Different assumptions on the size of the non-factorisable power corrections*

> Filled area: 10% power correction
> Solid contour: 60% power correction

"Guesstimate" of unknown power corrections:

Leading Order QCDf of non-factorisable piece $\times \left(1 + a_k \exp(i\phi_k) + b_k \frac{q^2}{6\,\mathrm{GeV}^2} \exp(i\theta_k)\right)$

with $a_k(b_k)$ varied between $-X\%(\times 2.5)$ and $+X\%(\times 2.5)$

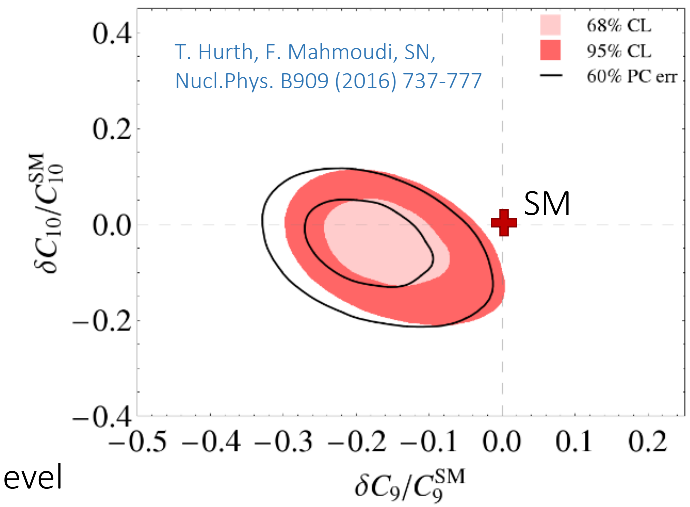

- Tension not significantly reduced with 60% power correction
- 60% power corrections at amplitude level $\Longrightarrow$ 17-20% on the observable level
- Large enough hadronic power corrections required to remove tension amount to more than 150% at the amplitude level in the critical bins (20-50% on the observable level)

NP effect vs. hadronic contributions

Instead of making assumptions on the size of the power corrections h_λ, they can be parameterised by a general ansatz (compatible with the analyticity structure): [Jäger, Camalich, 1412.3183], [Ciuchini et al. 1512.07157]

$$h_{\pm,[0]} = \left[\sqrt{q^2}\times\right]\left(h^{(0)}_{\pm,[0]} + q^2\, h^{(1)}_{\pm,[0]} + q^4\, h^{(2)}_{\pm,[0]}\right)$$

$\Longrightarrow$ NP effects in C_9 are embedded in the hadronic contributions [A. Arbey, T. Hurth, F. Mahmoudi, SN, 1806.02791]

Due to the embedding, fits to NP and hadronic contributions can be compared with the Wilks' test

Fit to

- Wilson coefficient $\delta C_9^{\rm NP}$
- Hadronic quantities $h^{(0,1,2)}_{+,-,0}$ (18 parameters)

$B \to K^*\mu^+\mu^-$ observables (low q^2) and BR($B \to K^*\gamma$)

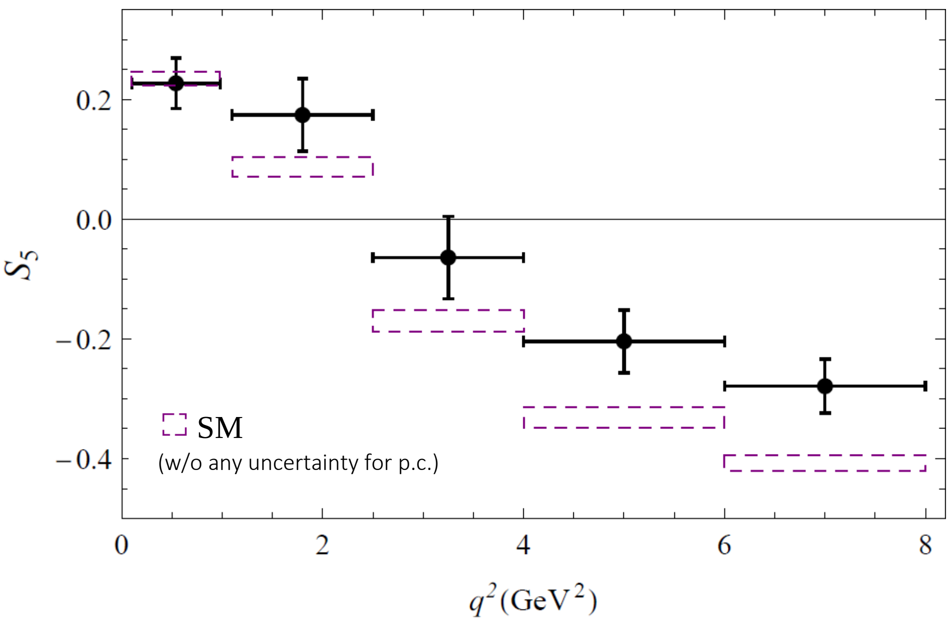

NP effect vs. hadronic contributions

Instead of making assumptions on the size of the power corrections h_λ, they can be parameterised by a general ansatz (compatible with the analyticity structure): [Jäger, Camalich, 1412.3183], [Ciuchini et al. 1512.07157]

$$h_{\pm,[0]} = \left[\sqrt{q^2}\times\right]\left(h^{(0)}_{\pm,[0]} + q^2\, h^{(1)}_{\pm,[0]} + q^4\, h^{(2)}_{\pm,[0]}\right)$$

$\Longrightarrow$ NP effects in C_9 are embedded in the hadronic contributions A. Arbey, T. Hurth, F. Mahmoudi, SN, 1806.02791]

Due to the embedding, fits to NP and hadronic contributions can be compared with the Wilks' test

Fit to
- Wilson coefficient $\delta C_9^{\rm NP}$
- Hadronic quantities $h^{(0,1,2)}_{+,-,0}$ (18 parameters)

$B \to K^*\mu^+\mu^-$ observables (low q^2) and BR($B \to K^*\gamma$)		
	Real δC_9 (1)	Hadronic fit (18)
Plain SM	6.0σ	4.7σ

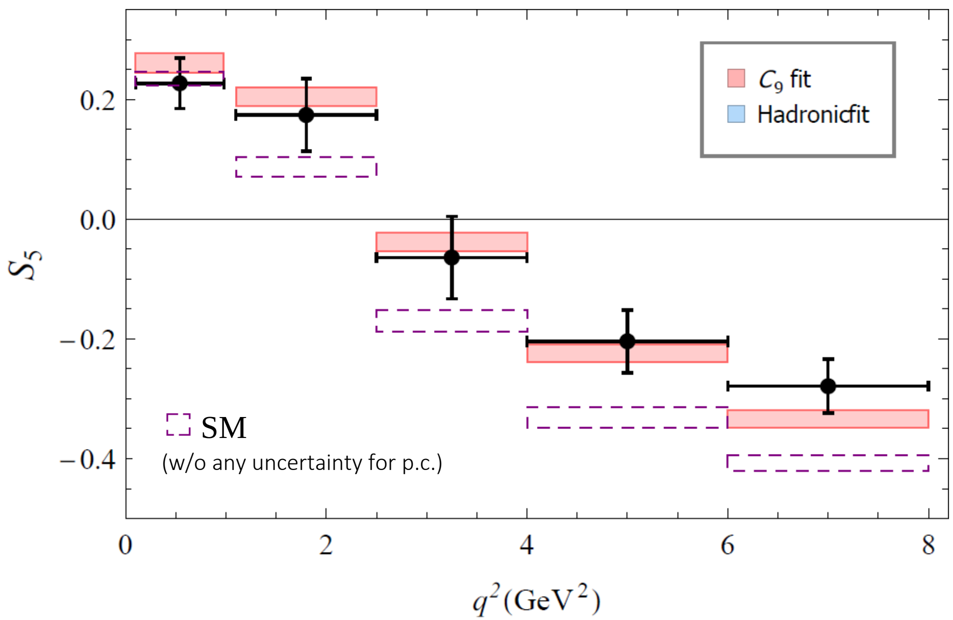

➤ Fit to δC_9 improves description of the data with 6σ compared to the SM (w/o any uncertainty for p.c.)

NP effect vs. hadronic contributions

Instead of making assumptions on the size of the power corrections h_λ, they can be parameterised by a general ansatz (compatible with the analyticity structure): [Jäger, Camalich, 1412.3183], [Ciuchini et al. 1512.07157]

$$h_{\pm,[0]} = \left[\sqrt{q^2}\times\right]\left(h^{(0)}_{\pm,[0]} + q^2\, h^{(1)}_{\pm,[0]} + q^4\, h^{(2)}_{\pm,[0]}\right)$$

$\Longrightarrow$ NP effects in C_9 are embedded in the hadronic contributions A. Arbey, T. Hurth, F. Mahmoudi, SN, 1806.02791]

Due to the embedding, fits to NP and hadronic contributions can be compared with the Wilks' test

Fit to
- Wilson coefficient $\delta C_9^{\rm NP}$
- Hadronic quantities $h^{(0,1,2)}_{+,-,0}$ (18 parameters)

$B \to K^*\mu^+\mu^-$ observables (low q^2) and BR($B \to K^*\gamma$)	Real δC_9 (1)	Hadronic fit (18)
Plain SM	6.0σ	4.7σ

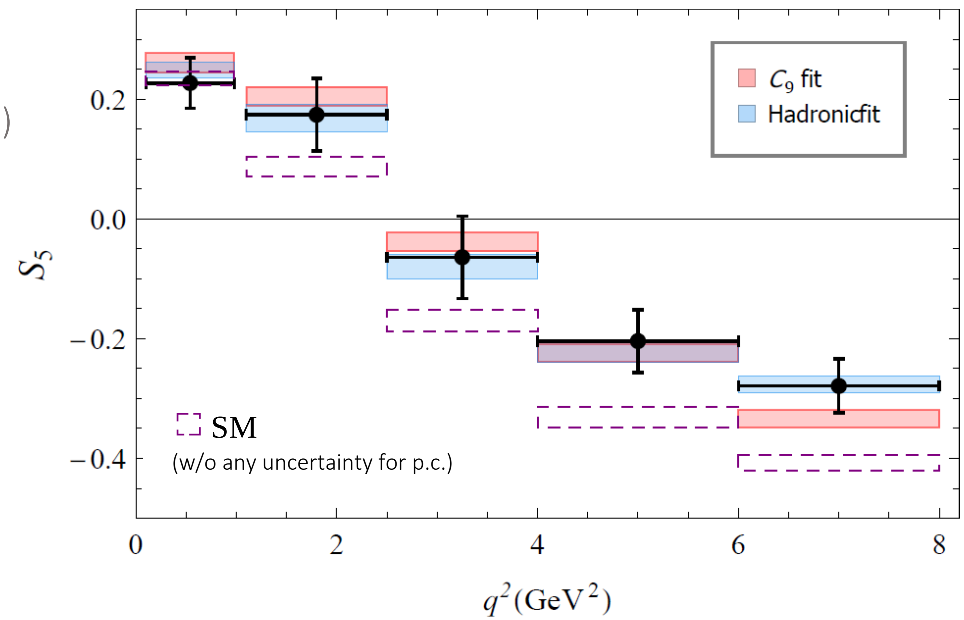

- Fit to δC_9 improves description of the data with 6σ compared to the SM (w/o any uncertainty for p.c.)
- Hadronic fit also describes the data well

NP effect vs. hadronic contributions

Instead of making assumptions on the size of the power corrections h_λ, they can be parameterised by a general ansatz (compatible with the analyticity structure): [Jäger, Camalich, 1412.3183], [Ciuchini et al. 1512.07157]

$$h_{\pm,[0]} = \left[\sqrt{q^2}\times\right]\left(h^{(0)}_{\pm,[0]} + q^2\, h^{(1)}_{\pm,[0]} + q^4\, h^{(2)}_{\pm,[0]}\right)$$

$\Longrightarrow$ NP effects in C_9 are embedded in the hadronic contributions A. Arbey, T. Hurth, F. Mahmoudi, SN, 1806.02791]

Due to the embedding, fits to NP and hadronic contributions can be compared with the Wilks' test

Fit to
- Wilson coefficient $\delta C_9^{\rm NP}$
- Hadronic quantities $h^{(0,1,2)}_{+,-,0}$ (18 parameters)

$B \to K^*\mu^+\mu^-$ observables (low q^2) and BR($B \to K^*\gamma$)		
	Real δC_9 (1)	Hadronic fit (18)
Plain SM	6.0σ	4.7σ
Real δC_9	--	1.5σ

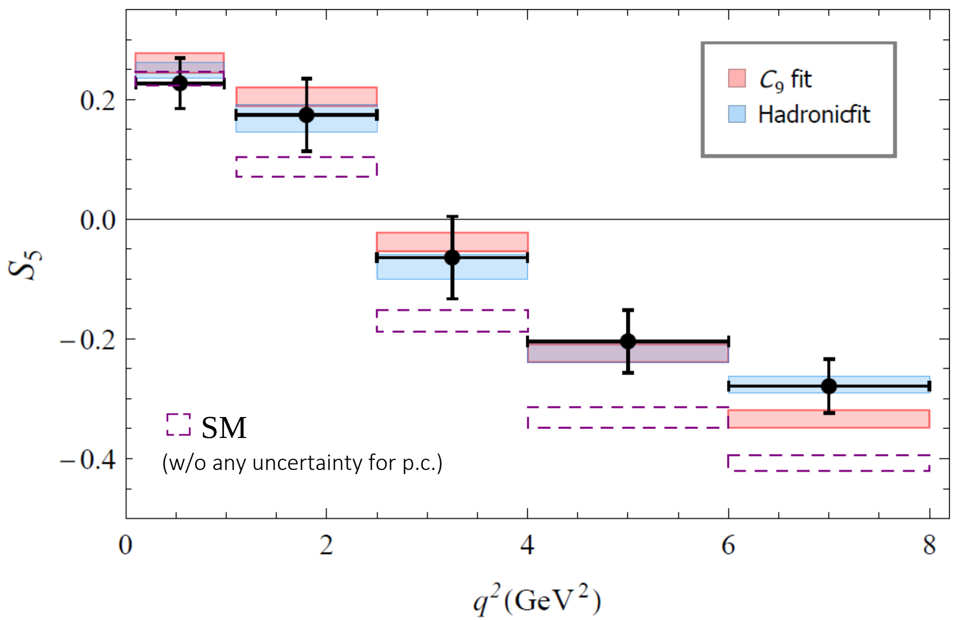

- Fit to δC_9 improves description of the data with 6σ compared to the SM (w/o any uncertainty for p.c.)
- Hadronic fit also describes the data well
- Adding 17 more parameters compared to the NP in C_9 doesn't significantly improve the fit ($\sim 1.5\sigma$)

NP fit vs. hadronic fit

The hadronic fit includes 18 free parameters

$B \to K^* \bar{\mu}\mu/\gamma$ observables ($\chi^2_{\rm SM} = 85.15,\ \chi^2_{\rm min} = 25.96;\ {\rm Pull}_{\rm SM} = 4.7\sigma$)		
	Real	Imaginary
$h_+^{(0)}$	$(-2.37 \pm 13.50) \times 10^{-5}$	$(7.86 \pm 13.79) \times 10^{-5}$
$h_+^{(1)}$	$(1.09 \pm 1.81) \times 10^{-4}$	$(1.58 \pm 1.69) \times 10^{-4}$
$h_+^{(2)}$	$(-1.10 \pm 2.66) \times 10^{-5}$	$(-2.45 \pm 2.51) \times 10^{-5}$
$h_-^{(0)}$	$(1.43 \pm 12.85) \times 10^{-5}$	$(-2.34 \pm 3.09) \times 10^{-4}$
$h_-^{(1)}$	$(-3.99 \pm 8.11) \times 10^{-5}$	$(1.44 \pm 2.82) \times 10^{-4}$
$h_-^{(2)}$	$(2.04 \pm 1.16) \times 10^{-5}$	$(-3.25 \pm 3.98) \times 10^{-5}$
$h_0^{(0)}$	$(2.38 \pm 2.43) \times 10^{-4}$	$(5.10 \pm 3.18) \times 10^{-4}$
$h_0^{(1)}$	$(1.40 \pm 1.98) \times 10^{-4}$	$(-1.66 \pm 2.41) \times 10^{-4}$
$h_0^{(2)}$	$(-1.57 \pm 2.43) \times 10^{-5}$	$(3.04 \pm 29.87) \times 10^{-6}$

The hadronic fit includes 18 free parameters

$B \to K^* \bar{\mu}\mu/\gamma$ observables ($\chi^2_{\rm SM} = 85.15,\ \chi^2_{\rm min} = 25.96;\ {\rm Pull}_{\rm SM} = 4.7\sigma$)		
	Real	Imaginary
$h_+^{(0)}$	$(-2.37 \pm 13.50) \times 10^{-5}$	$(7.86 \pm 13.79) \times 10^{-5}$
$h_+^{(1)}$	$(1.09 \pm 1.81) \times 10^{-4}$	$(1.58 \pm 1.69) \times 10^{-4}$
$h_+^{(2)}$	$(-1.10 \pm 2.66) \times 10^{-5}$	$(-2.45 \pm 2.51) \times 10^{-5}$
$h_-^{(0)}$	$(1.43 \pm 12.85) \times 10^{-5}$	$(-2.34 \pm 3.09) \times 10^{-4}$
$h_-^{(1)}$	$(-3.99 \pm 8.11) \times 10^{-5}$	$(1.44 \pm 2.82) \times 10^{-4}$
$h_-^{(2)}$	$(2.04 \pm 1.16) \times 10^{-5}$	$(-3.25 \pm 3.98) \times 10^{-5}$
$h_0^{(0)}$	$(2.38 \pm 2.43) \times 10^{-4}$	$(5.10 \pm 3.18) \times 10^{-4}$
$h_0^{(1)}$	$(1.40 \pm 1.98) \times 10^{-4}$	$(-1.66 \pm 2.41) \times 10^{-4}$
$h_0^{(2)}$	$(-1.57 \pm 2.43) \times 10^{-5}$	$(3.04 \pm 29.87) \times 10^{-6}$

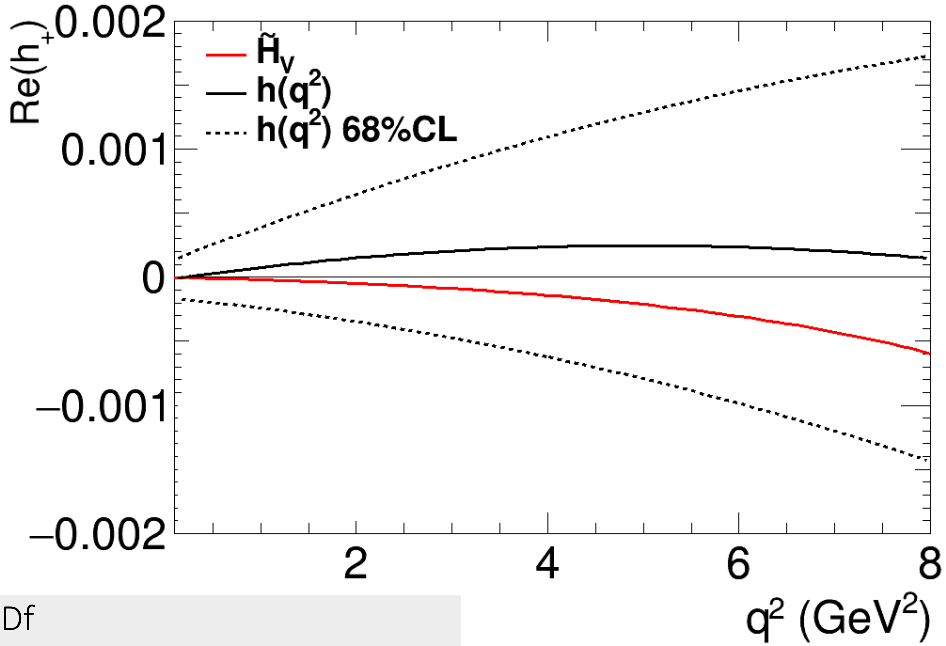

Red line: LO QCDf
Solid black line: h_λ
Dashed black line: 68% C.L. region of h_λ fit

- ➢ h_λ compatible with zero at 1σ level

⟶ too many free parameters to get strongly constrained with current data

NP fit vs. hadronic fit

The hadronic fit includes 18 free parameters

$B \to K^* \bar{\mu}\mu/\gamma$ observables ($\chi^2_{\rm SM} = 85.15,\ \chi^2_{\rm min} = 25.96;\ {\rm Pull_{SM}} = 4.7\sigma$)		
	Real	Imaginary
$h_+^{(0)}$	$(-2.37 \pm 13.50) \times 10^{-5}$	$(7.86 \pm 13.79) \times 10^{-5}$
$h_+^{(1)}$	$(1.09 \pm 1.81) \times 10^{-4}$	$(1.58 \pm 1.69) \times 10^{-4}$
$h_+^{(2)}$	$(-1.10 \pm 2.66) \times 10^{-5}$	$(-2.45 \pm 2.51) \times 10^{-5}$
$h_-^{(0)}$	$(1.43 \pm 12.85) \times 10^{-5}$	$(-2.34 \pm 3.09) \times 10^{-4}$
$h_-^{(1)}$	$(-3.99 \pm 8.11) \times 10^{-5}$	$(1.44 \pm 2.82) \times 10^{-4}$
$h_-^{(2)}$	$(2.04 \pm 1.16) \times 10^{-5}$	$(-3.25 \pm 3.98) \times 10^{-5}$
$h_0^{(0)}$	$(2.38 \pm 2.43) \times 10^{-4}$	$(5.10 \pm 3.18) \times 10^{-4}$
$h_0^{(1)}$	$(1.40 \pm 1.98) \times 10^{-4}$	$(-1.66 \pm 2.41) \times 10^{-4}$
$h_0^{(2)}$	$(-1.57 \pm 2.43) \times 10^{-5}$	$(3.04 \pm 29.87) \times 10^{-6}$

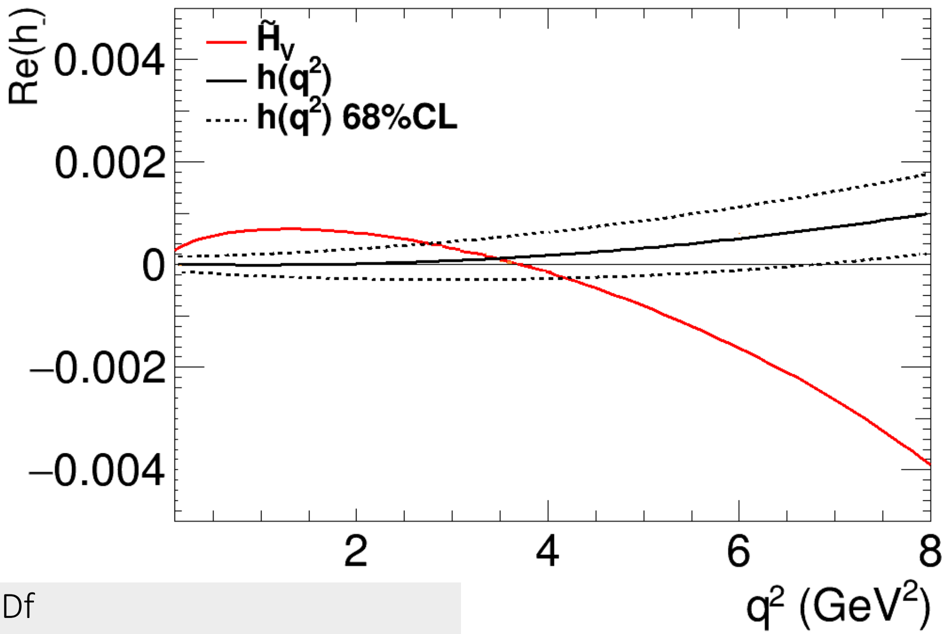

Red line: LO QCDf
Solid black line: h_λ
Dashed black line: 68% C.L. region of h_λ fit

- h_λ compatible with zero at 1σ level

$\longrightarrow$ too many free parameters to get strongly constrained with current data

The hadronic fit includes 18 free parameters

$B \to K^* \bar{\mu}\mu/\gamma$ observables ($\chi^2_{\rm SM} = 85.15,\ \chi^2_{\rm min} = 25.96;\ {\rm Pull}_{\rm SM} = 4.7\sigma$)		
	Real	Imaginary
$h_+^{(0)}$	$(-2.37 \pm 13.50) \times 10^{-5}$	$(7.86 \pm 13.79) \times 10^{-5}$
$h_+^{(1)}$	$(1.09 \pm 1.81) \times 10^{-4}$	$(1.58 \pm 1.69) \times 10^{-4}$
$h_+^{(2)}$	$(-1.10 \pm 2.66) \times 10^{-5}$	$(-2.45 \pm 2.51) \times 10^{-5}$
$h_-^{(0)}$	$(1.43 \pm 12.85) \times 10^{-5}$	$(-2.34 \pm 3.09) \times 10^{-4}$
$h_-^{(1)}$	$(-3.99 \pm 8.11) \times 10^{-5}$	$(1.44 \pm 2.82) \times 10^{-4}$
$h_-^{(2)}$	$(2.04 \pm 1.16) \times 10^{-5}$	$(-3.25 \pm 3.98) \times 10^{-5}$
$h_0^{(0)}$	$(2.38 \pm 2.43) \times 10^{-4}$	$(5.10 \pm 3.18) \times 10^{-4}$
$h_0^{(1)}$	$(1.40 \pm 1.98) \times 10^{-4}$	$(-1.66 \pm 2.41) \times 10^{-4}$
$h_0^{(2)}$	$(-1.57 \pm 2.43) \times 10^{-5}$	$(3.04 \pm 29.87) \times 10^{-6}$

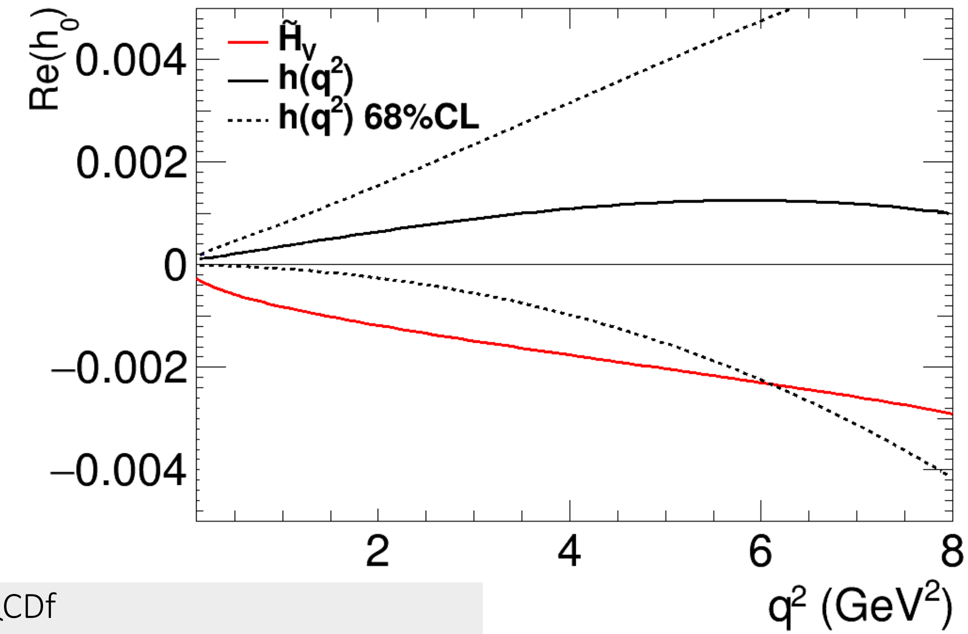

Red line: LO QCDf
Solid black line: h_λ
Dashed black line: 68% C.L. region of h_λ fit

- h_λ compatible with zero at 1σ level

⟶ too many free parameters to get strongly constrained with current data

The hadronic fit includes 18 free parameters

$B \to K^* \bar{\mu}\mu/\gamma$ observables ($\chi^2_{\rm SM} = 85.15,\ \chi^2_{\rm min} = 25.96;\ {\rm Pull_{SM}} = 4.7\sigma$)		
	Real	Imaginary
$h_+^{(0)}$	$(-2.37 \pm 13.50) \times 10^{-5}$	$(7.86 \pm 13.79) \times 10^{-5}$
$h_+^{(1)}$	$(1.09 \pm 1.81) \times 10^{-4}$	$(1.58 \pm 1.69) \times 10^{-4}$
$h_+^{(2)}$	$(-1.10 \pm 2.66) \times 10^{-5}$	$(-2.45 \pm 2.51) \times 10^{-5}$
$h_-^{(0)}$	$(1.43 \pm 12.85) \times 10^{-5}$	$(-2.34 \pm 3.09) \times 10^{-4}$
$h_-^{(1)}$	$(-3.99 \pm 8.11) \times 10^{-5}$	$(1.44 \pm 2.82) \times 10^{-4}$
$h_-^{(2)}$	$(2.04 \pm 1.16) \times 10^{-5}$	$(-3.25 \pm 3.98) \times 10^{-5}$
$h_0^{(0)}$	$(2.38 \pm 2.43) \times 10^{-4}$	$(5.10 \pm 3.18) \times 10^{-4}$
$h_0^{(1)}$	$(1.40 \pm 1.98) \times 10^{-4}$	$(-1.66 \pm 2.41) \times 10^{-4}$
$h_0^{(2)}$	$(-1.57 \pm 2.43) \times 10^{-5}$	$(3.04 \pm 29.87) \times 10^{-6}$

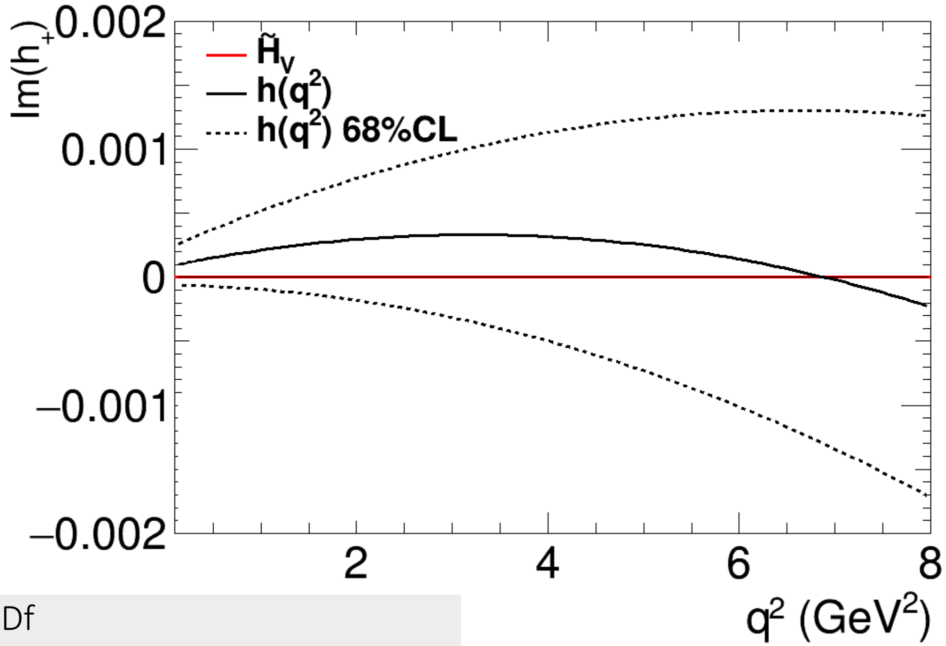

Red line: LO QCDf
Solid black line: h_λ
Dashed black line: 68% C.L. region of h_λ fit

- h_λ compatible with zero at 1σ level

⟶ too many free parameters to get strongly constrained with current data

NP fit vs. hadronic fit

The hadronic fit includes 18 free parameters

$B \to K^* \bar{\mu}\mu/\gamma$ observables ($\chi^2_{\rm SM} = 85.15$, $\chi^2_{\rm min} = 25.96$; ${\rm Pull}_{\rm SM} = 4.7\sigma$)		
	Real	Imaginary
$h_+^{(0)}$	$(-2.37 \pm 13.50) \times 10^{-5}$	$(7.86 \pm 13.79) \times 10^{-5}$
$h_+^{(1)}$	$(1.09 \pm 1.81) \times 10^{-4}$	$(1.58 \pm 1.69) \times 10^{-4}$
$h_+^{(2)}$	$(-1.10 \pm 2.66) \times 10^{-5}$	$(-2.45 \pm 2.51) \times 10^{-5}$
$h_-^{(0)}$	$(1.43 \pm 12.85) \times 10^{-5}$	$(-2.34 \pm 3.09) \times 10^{-4}$
$h_-^{(1)}$	$(-3.99 \pm 8.11) \times 10^{-5}$	$(1.44 \pm 2.82) \times 10^{-4}$
$h_-^{(2)}$	$(2.04 \pm 1.16) \times 10^{-5}$	$(-3.25 \pm 3.98) \times 10^{-5}$
$h_0^{(0)}$	$(2.38 \pm 2.43) \times 10^{-4}$	$(5.10 \pm 3.18) \times 10^{-4}$
$h_0^{(1)}$	$(1.40 \pm 1.98) \times 10^{-4}$	$(-1.66 \pm 2.41) \times 10^{-4}$
$h_0^{(2)}$	$(-1.57 \pm 2.43) \times 10^{-5}$	$(3.04 \pm 29.87) \times 10^{-6}$

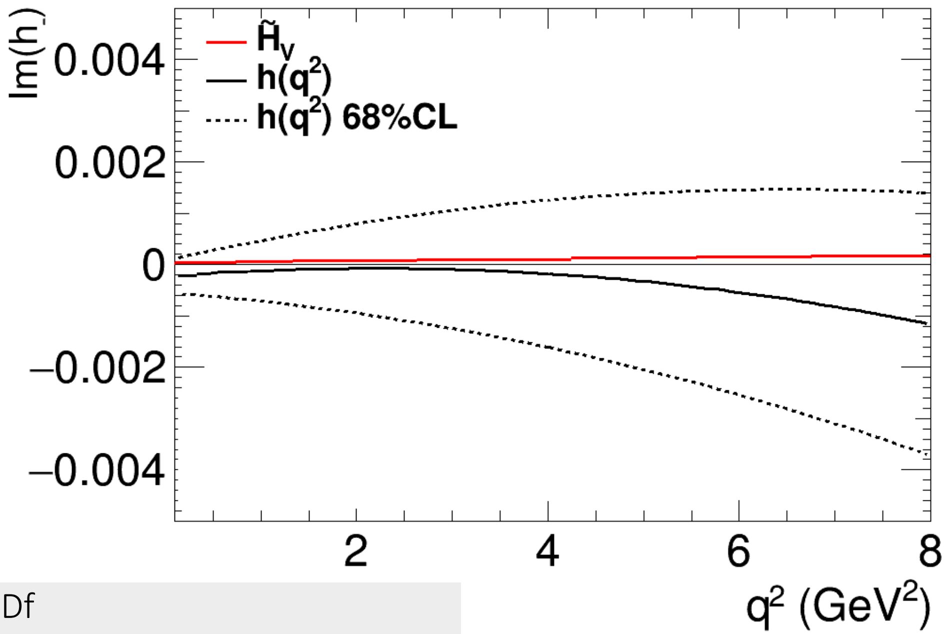

Red line: LO QCDf
Solid black line: h_λ
Dashed black line: 68% C.L. region of h_λ fit

- h_λ compatible with zero at 1σ level

⟶ too many free parameters to get strongly constrained with current data

NP fit vs. hadronic fit

The hadronic fit includes 18 free parameters

$B \to K^* \bar{\mu}\mu/\gamma$ observables ($\chi^2_{\rm SM} = 85.15,\ \chi^2_{\rm min} = 25.96;\ {\rm Pull}_{\rm SM} = 4.7\sigma$)		
	Real	Imaginary
$h_+^{(0)}$	$(-2.37 \pm 13.50) \times 10^{-5}$	$(7.86 \pm 13.79) \times 10^{-5}$
$h_+^{(1)}$	$(1.09 \pm 1.81) \times 10^{-4}$	$(1.58 \pm 1.69) \times 10^{-4}$
$h_+^{(2)}$	$(-1.10 \pm 2.66) \times 10^{-5}$	$(-2.45 \pm 2.51) \times 10^{-5}$
$h_-^{(0)}$	$(1.43 \pm 12.85) \times 10^{-5}$	$(-2.34 \pm 3.09) \times 10^{-4}$
$h_-^{(1)}$	$(-3.99 \pm 8.11) \times 10^{-5}$	$(1.44 \pm 2.82) \times 10^{-4}$
$h_-^{(2)}$	$(2.04 \pm 1.16) \times 10^{-5}$	$(-3.25 \pm 3.98) \times 10^{-5}$
$h_0^{(0)}$	$(2.38 \pm 2.43) \times 10^{-4}$	$(5.10 \pm 3.18) \times 10^{-4}$
$h_0^{(1)}$	$(1.40 \pm 1.98) \times 10^{-4}$	$(-1.66 \pm 2.41) \times 10^{-4}$
$h_0^{(2)}$	$(-1.57 \pm 2.43) \times 10^{-5}$	$(3.04 \pm 29.87) \times 10^{-6}$

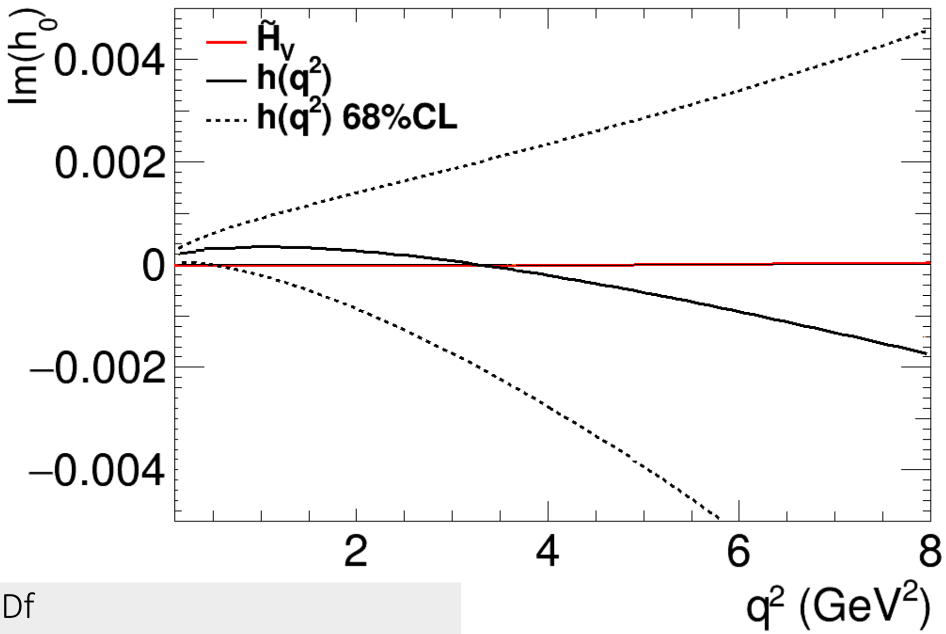

Red line: LO QCDf
Solid black line: h_λ
Dashed black line: 68% C.L. region of h_λ fit

- h_λ compatible with zero at 1σ level

⟶ too many free parameters to get strongly constrained with current data

NP fit vs. hadronic fit

A (minimal) description of hadronic contributions with fewer free parameters

$$h_\lambda(q^2) = -\frac{\tilde{V}_\lambda(q^2)}{16\pi^2}\frac{q^2}{m_B^2}\Delta C_9^{\lambda,\mathrm{PC}}$$

for each helicity ($\lambda = +,-,0$) a different ΔC_9^{PC}
→ three real (six complex) parameters

- If NP in C_9 is the favoured scenario, the three different fitted helicities should give the same value
  ⇒ Can work as a null test for NP

NP fit vs. hadronic fit

A (minimal) description of hadronic contributions with fewer free parameters

$$h_\lambda(q^2) = -\frac{\tilde{V}_\lambda(q^2)}{16\pi^2}\frac{q^2}{m_B^2}\Delta C_9^{\lambda,\mathrm{PC}}$$

for each helicity ($\lambda = +,-,0$) a different ΔC_9^{PC}
→ three real (six complex) parameters

- If NP in C_9 is the favoured scenario, the three different fitted helicities should give the same value
  ⇒ Can work as a null test for NP

$B \to K^* \bar{\mu}\mu/\gamma$ observables ($\chi^2_{\mathrm{SM}} = 85.15,\ \chi^2_{\min} = 39.40;\ \mathrm{Pull}_{\mathrm{SM}} = 5.5\sigma$)	
	best fit value
$\Delta C_9^{+,\mathrm{PC}}$	$(3.39 \pm 6.44) + i(-14.98 \pm 8.40)$
$\Delta C_9^{-,\mathrm{PC}}$	$(-1.02 \pm 0.22) + i(-0.68 \pm 0.79)$
$\Delta C_9^{0,\mathrm{PC}}$	$(-0.83 \pm 0.53) + i(-0.89 \pm 0.69)$

Fitted parameters not the same for different helicities but in agreement with each other within 1σ

NP fit vs. hadronic fit

A (minimal) description of hadronic contributions with fewer free parameters

$$h_\lambda(q^2) = -\frac{\tilde{V}_\lambda(q^2)}{16\pi^2}\frac{q^2}{m_B^2}\Delta C_9^{\lambda,\mathrm{PC}}$$

for each helicity ($\lambda = +,-,0$) a different ΔC_9^{PC}
→ three real (six complex) parameters

- If NP in C_9 is the favoured scenario, the three different fitted helicities should give the same value
  ⇒ Can work as a null test for NP

$B \to K^* \bar{\mu}\mu/\gamma$ observables ($\chi^2_{\mathrm{SM}} = 85.15,\ \chi^2_{\min} = 39.40;\ \mathrm{Pull}_{\mathrm{SM}} = 5.5\sigma$)	
	best fit value
$\Delta C_9^{+,\mathrm{PC}}$	$(3.39 \pm 6.44) + i(-14.98 \pm 8.40)$
$\Delta C_9^{-,\mathrm{PC}}$	$(-1.02 \pm 0.22) + i(-0.68 \pm 0.79)$
$\Delta C_9^{0,\mathrm{PC}}$	$(-0.83 \pm 0.53) + i(-0.89 \pm 0.69)$

Fitted parameters not the same for different helicities but in agreement with each other within 1σ

Fit to only BR($B \to K^*\gamma$) and $B \to K^*\mu^+\mu^-$ observables (low q^2)		
	Real δC_9 (1)	Hadronic fit; Complex $\Delta C_9^{\lambda,\mathrm{PC}}$ (6)
Plain SM (0)	(6.0σ)	(5.5σ)
Real δC_9 (1)	--	(1.8σ)

- Adding the hadronic parameters improve the fit with less than 2σ significance

Strong indication that the NP interpretation is a valid option, although the situation remains inconclusive

Prospects for hadronic fit to $B \to K^*\mu\mu$

LHCb projections for $B \to K^* \mu^+ \mu^-$ with 14, 50 and 300 fb^{-1} luminosity

Keeping present central values, the three benchmark points don't give acceptable fits (p-value ≈ 0)

We assume two extreme scenarios, adjusting the experimental data such that

- Central value of fit to C_9 remains the same
- Central values of the hadronic fit remain the same

Future prospect

LHCb projections for $B \to K^{*}\mu^{+}\mu^{-}$ with 14, 50 and 300 fb^{-1} luminosity

Keeping present central values, the three benchmark points don't give acceptable fits (p-value ≈ 0)

We assume two extreme scenarios, adjusting the experimental data such that

- Central value of fit to C_9 remains the same
- Central values of the hadronic fit remain the same

Central value of fit to C_9 remains the same						
	14 fb^{-1} (Syst.)		50 fb^{-1} (Syst./4)		300 fb^{-1} (Syst./4)	
	Real δC_9	Hadronic fit h_λ	Real δC_9	Hadronic fit h_λ	Real δC_9	Hadronic fit h_λ
Plain SM	8.1σ	5.1σ	15.1σ	12.9σ	21.4σ	19.6σ

- Very good fits for C_9 by construction

Future prospect

LHCb projections for $B \to K^* \mu^+ \mu^-$ with 14, 50 and 300 fb^{-1} luminosity

Keeping present central values, the three benchmark points don't give acceptable fits (p-value ≈ 0)

We assume two extreme scenarios, adjusting the experimental data such that

- ❑ Central value of fit to C_9 remains the same
- ❑ Central values of the hadronic fit remain the same

Central value of fit to C_9 remains the same						
	14 fb^{-1} (Syst.)		**50 fb^{-1} (Syst./4)**		**300 fb^{-1} (Syst./4)**	
	Real δC_9	Hadronic fit h_λ	Real δC_9	Hadronic fit h_λ	Real δC_9	Hadronic fit h_λ
Plain SM	8.1σ	5.1σ	15.1σ	12.9σ	21.4σ	19.6σ

- ➢ Very good fits for C_9 by construction
- ➢ Good hadronic fits for all three benchmark points of this scenario, but no improvement compared to C_9
- ↪ Uncertainties of most of the parameters of the hadronic fit become very large for higher luminosities indicating most of the 18 parameters are not needed to describe the data

Future prospect

LHCb projections for $B \to K^*\mu^+\mu^-$ with 14, 50 and 300 fb^{-1} luminosity

Keeping present central values, the three benchmark points don't give acceptable fits (p-value ≈ 0)

We assume two extreme scenarios, adjusting the experimental data such that

- ❑ Central value of fit to C_9 remains the same
- ❑ Central values of the hadronic fit remain the same

Central values of the hadronic fit is always the same						
	14 fb^{-1} (Syst.)		**50 fb^{-1} (Syst./4)**		**300 fb^{-1} (Syst./4)**	
	Real δC_9	Hadronic fit h_λ	Real δC_9	Hadronic fit h_λ	Real δC_9	Hadronic fit h_λ
Plain SM	7.9σ	7.9σ	14.6σ	22.5σ	18.9σ	41.8σ

Future prospect

LHCb projections for $B \to K^* \mu^+ \mu^-$ with 14, 50 and 300 fb^{-1} luminosity

Keeping present central values, the three benchmark points don't give acceptable fits (p-value ≈ 0)

We assume two extreme scenarios, adjusting the experimental data such that

- ❑ Central value of fit to C_9 remains the same
- ❑ Central values of the hadronic fit remain the same

Central values of the hadronic fit is always the same						
	14 fb^{-1} (Syst.)		**50 fb^{-1} (Syst./4)**		**300 fb^{-1} (Syst./4)**	
	Real δC_9	Hadronic fit h_λ	Real δC_9	Hadronic fit h_λ	Real δC_9	Hadronic fit h_λ
Plain SM	7.9σ	7.9σ	14.6σ	22.5σ	18.9σ	41.8σ
Real δC_9	--	4.0σ	--	17.5σ	--	37.4σ

- Hadronic fit, gives an improvement with 4σ significance compared to fit to C_9 after Run 2 (14 fb^{-1}) but situation still remains inconclusive
- After first LHCb upgrade (50 fb^{-1}) conclusive judgment is possible

Future prospect

LHCb projections for $B \to K^*\mu^+\mu^-$ with 14, 50 and 300 fb^{-1} luminosity

Keeping present central values, the three benchmark points don't give acceptable fits (p-value ≈ 0)

We assume two extreme scenarios, adjusting the experimental data such that

- ❑ Central value of fit to C_9 remains the same
- ❑ Central values of the hadronic fit remain the same

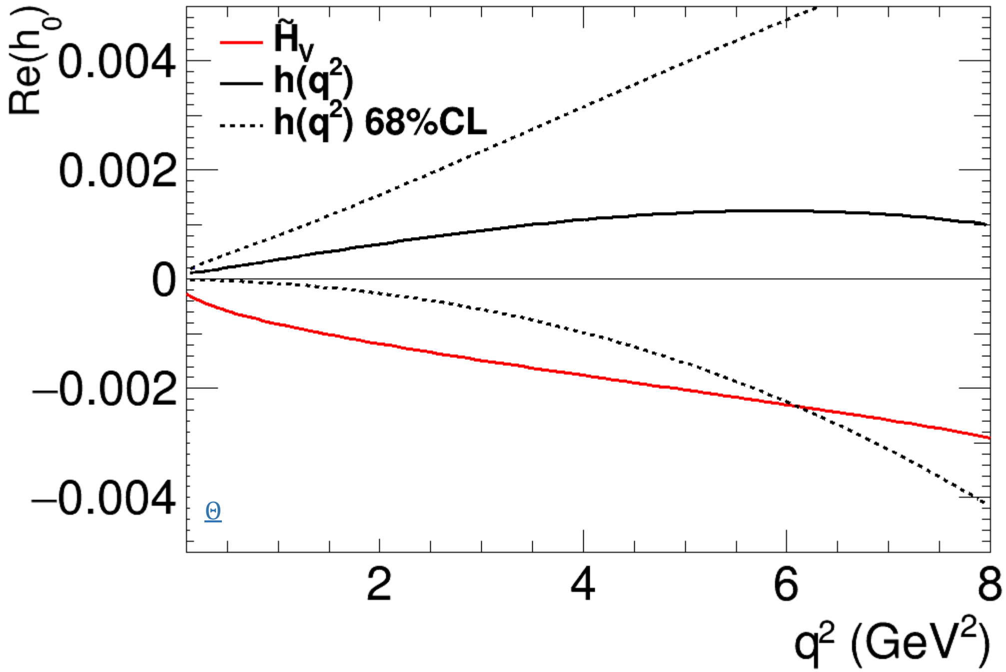

- Hadronic fit, gives an improvement with 4σ significance compared to fit to C_9 after Run 2 (14 fb^{-1}) but situation still remains inconclusive
- After first LHCb upgrade (50 fb^{-1}) conclusive judgment is possible

Future prospect

LHCb projections for $B \to K^* \mu^+ \mu^-$ with 14, 50 and 300 fb^{-1} luminosity

Keeping present central values, the three benchmark points don't give acceptable fits (p-value ≈ 0)

We assume two extreme scenarios, adjusting the experimental data such that

- ❑ Central value of fit to C_9 remains the same
- ❑ Central values of the hadronic fit remain the same

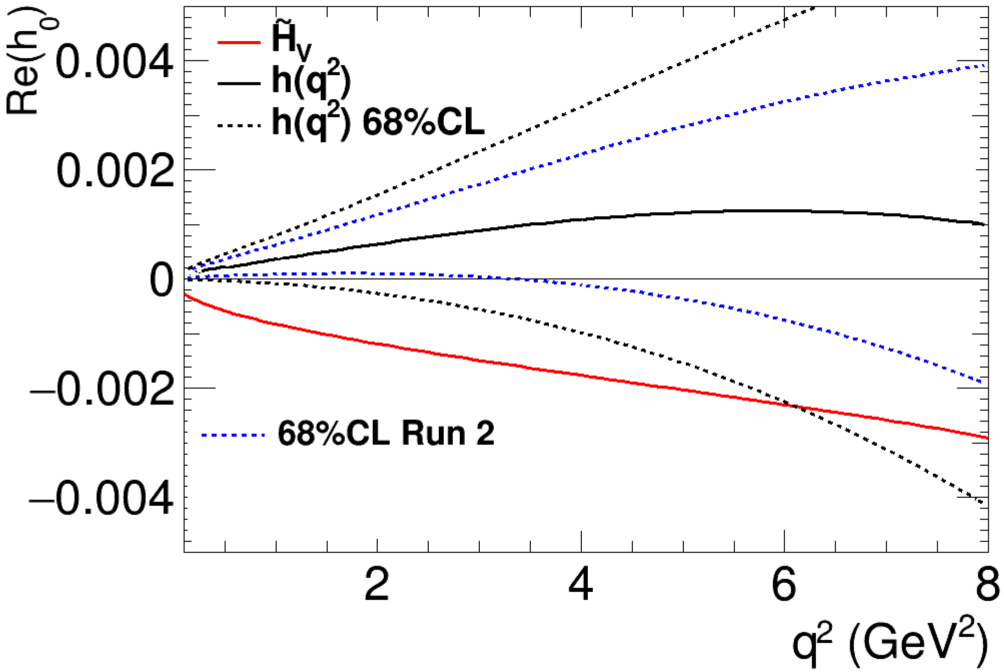

- Hadronic fit, gives an improvement with 4σ significance compared to fit to C_9 after Run 2 (14 fb^{-1}) but situation still remains inconclusive
- After first LHCb upgrade (50 fb^{-1}) conclusive judgment is possible

Future prospect

LHCb projections for $B \to K^*\mu^+\mu^-$ with 14, 50 and 300 fb^{-1} luminosity

Keeping present central values, the three benchmark points don't give acceptable fits (p-value ≈ 0)

We assume two extreme scenarios, adjusting the experimental data such that

- ❑ Central value of fit to C_9 remains the same
- ❑ Central values of the hadronic fit remain the same

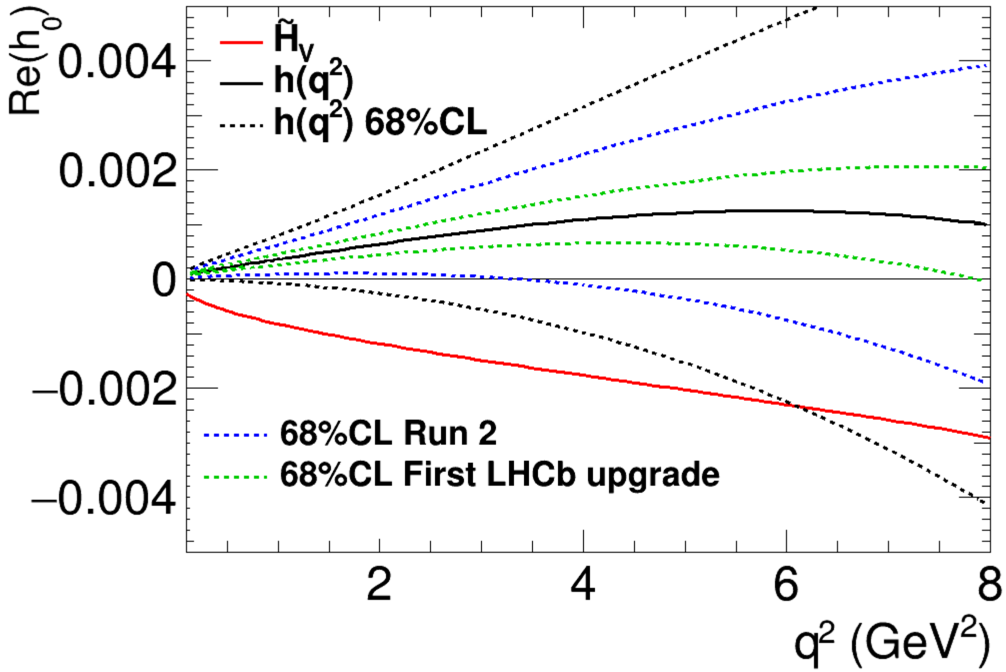

- Hadronic fit, gives an improvement with 4σ significance compared to fit to C_9 after Run 2 (14 fb^{-1}) but situation still remains inconclusive
- After first LHCb upgrade (50 fb^{-1}) conclusive judgment is possible
  ↪ fitted parameters no longer consistent with zero at 1σ level

Future prospect

LHCb projections for $B \to K^*\mu^+\mu^-$ with 14, 50 and 300 fb^{-1} luminosity

Keeping present central values, the three benchmark points don't give acceptable fits (p-value ≈ 0)

We assume two extreme scenarios, adjusting the experimental data such that

- ❑ Central value of fit to C_9 remains the same
- ❑ Central values of the hadronic fit remain the same

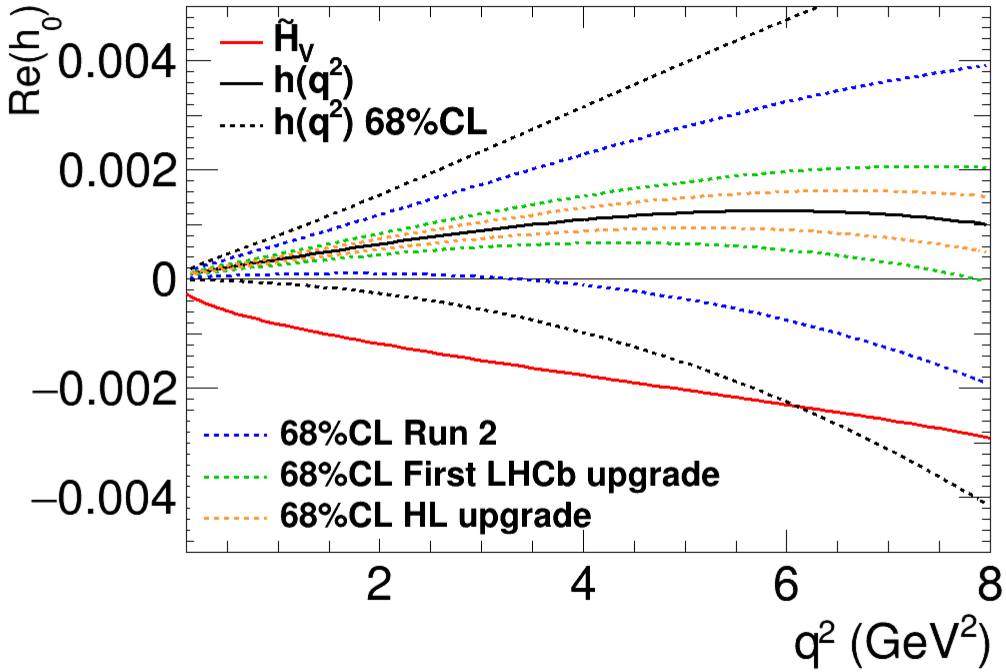

- Hadronic fit, gives an improvement with 4σ significance compared to fit to C_9 after Run 2 (14 fb^{-1}) but situation still remains inconclusive
- After first LHCb upgrade (50 fb^{-1}) conclusive judgment is possible
  ↪ fitted parameters no longer consistent with zero at 1σ level

$B \to V\ell\ell$ decay

Differential decay distribution

$$\frac{d^4\Gamma}{dq^2\, d\cos\theta_l\, d\cos\theta_K\, d\phi} = \frac{9}{32\pi} J(q^2, \theta_l, \theta_K, \phi)$$

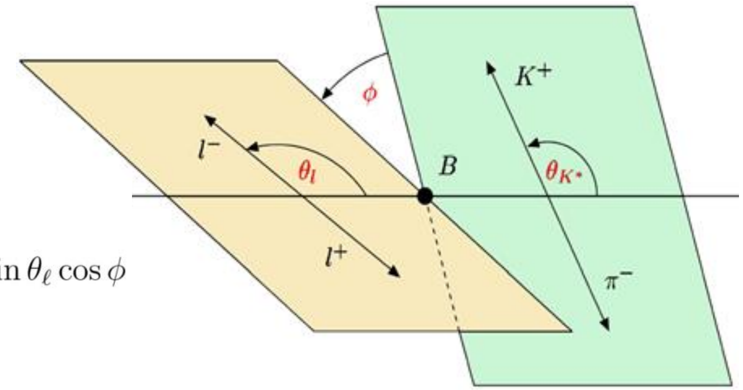

$$\begin{aligned} J(q^2, \theta_\ell, \theta_{K^*}, \phi) = {} & J_1^s \sin^2\theta_{K^*} + J_1^c \cos^2\theta_{K^*} + (J_2^s \sin^2\theta_{K^*} + J_2^c \cos^2\theta_{K^*}) \cos 2\theta_\ell \\ & + J_3 \sin^2\theta_{K^*} \sin^2\theta_\ell \cos 2\phi + J_4 \sin 2\theta_{K^*} \sin 2\theta_\ell \cos\phi + J_5 \sin 2\theta_{K^*} \sin\theta_\ell \cos\phi \\ & + (J_6^s \sin^2\theta_{K^*} + J_6^c \cos^2\theta_{K^*}) \cos\theta_\ell + J_7 \sin 2\theta_{K^*} \sin\theta_\ell \sin\phi \\ & + J_8 \sin 2\theta_{K^*} \sin 2\theta_\ell \sin\phi + J_9 \sin^2\theta_{K^*} \sin^2\theta_\ell \sin 2\phi \end{aligned}$$

Angular observables:

$$\langle P_1 \rangle_{\text{bin}} = \frac{1}{2} \frac{\int_{\text{bin}} dq^2 [J_3 + \bar{J}_3]}{\int_{\text{bin}} dq^2 [J_{2s} + \bar{J}_{2s}]}$$

$$\langle P_2 \rangle_{\text{bin}} = \frac{1}{8} \frac{\int_{\text{bin}} dq^2 [J_{6s} + \bar{J}_{6s}]}{\int_{\text{bin}} dq^2 [J_{2s} + \bar{J}_{2s}]}$$

$$\mathcal{N}'_{\text{bin}} = \sqrt{-\int_{\text{bin}} dq^2 [J_{2s} + \bar{J}_{2s}] \int_{\text{bin}} dq^2 [J_{2c} + \bar{J}_{2c}]}$$

$$\langle P'_4 \rangle_{\text{bin}} = \frac{1}{\mathcal{N}'_{\text{bin}}} \int_{\text{bin}} dq^2 [J_4 + \bar{J}_4]$$

$$\langle P'_5 \rangle_{\text{bin}} = \frac{1}{2\mathcal{N}'_{\text{bin}}} \int_{\text{bin}} dq^2 [J_5 + \bar{J}_5]$$

$$\langle P'_6 \rangle_{\text{bin}} = \frac{-1}{2\mathcal{N}'_{\text{bin}}} \int_{\text{bin}} dq^2 [J_7 + \bar{J}_7]$$

[Egede et al. 0807.2589]
[Egede et al. 1005.0571]
[Matias et al. 1202.4266]
[Descotes-Genon et al. 1303.5794]

$$S_i = (J_i + \bar{J}_i) \Big/ \left(\frac{d\Gamma}{dq^2} + \frac{d\bar{\Gamma}}{dq^2} \right)$$

[Altmannshofer et al. 0811.1214]